Unravelling the neurocognitive mechanisms underlying counterconditioning in humans

Lisa Wirz[1,2‡*], Maxime C. Houtekamer[1‡], Jette de Vos[3], Joseph E. Dunsmoor[4], Judith R. Homberg[1‡], Marloes J.A.G. Henckens[1‡], Erno J. Hermans[1]

[1] *Donders Institute for Brain, Cognition, and Behaviour, Radboud University Nijmegen Medical Center, Nijmegen, The Netherlands*

[2] *Cognitive Psychology, Ruhr University Bochum, Germany*

[3] *Department of Psychiatry and Neuropsychology, MHeNs, Maastricht University, The Netherlands*

[4] *Department of Psychiatry and Behavioral Sciences, University of Texas at Austin, United States*

‡ *These authors contributed equally to this work*

* Corresponding author:

Lisa Wirz
Email: lisa.wirz@donders.ru.nl
Phone: (+31) 024 361 1301
Kapittelweg 29, 6525 EN Nijmegen, The Netherlands

Short title: Neurocognitive mechanisms of counterconditioning

Keywords: Fear conditioning, counterconditioning, reward, ventral striatum, ventromedial prefrontal cortex

Abstract: 200 words

Main text (excl. abstract, methods, references, figure legends): 5517

N Figures: 6

N Tables: 1

Supplementary Information

Abstract

Counterconditioning (CC) aims to enhance extinction of threat memories by establishing new associations of opposite valence. While its underlying neurocognitive mechanisms remain largely unexplored, previous studies suggest qualitatively different mechanisms from regular extinction. In this functional MRI study, participants underwent categorical threat conditioning (CS+/CS-: images of animals/tools), followed by either CC (CS+ images reinforced with monetary rewards, n=24) or regular extinction (n=24). The following day, we assessed spontaneous recovery of threat responses and episodic memory for CS+ and CS- category exemplars. While the ventromedial prefrontal cortex (vmPFC) was activated during regular extinction, participants undergoing CC showed persistent CS+-specific deactivation of the vmPFC and hippocampus, and CS+-specific activation of the nucleus accumbens (NAcc). The following day, physiological threat responses returned in the regular extinction group, but not in the CC group. Counterconditioning furthermore strengthened episodic memory for CS+ exemplars presented during CC, and retroactively also for CS+ exemplars presented during the threat conditioning phase. Our findings confirm that CC leads to more persistent extinction of threat memories, as well as altered consolidation of the threat conditioning episode. Crucially, we show a qualitatively different activation pattern during CC versus regular extinction, with a shift away from the vmPFC and towards the NAcc.

Introduction

Trauma-related disorders are prevalent and highly detrimental to the individual's quality of life[1]. To treat these disorders, patients undergo exposure therapy in a safe therapeutic environment, causing threat responses to fade away[2]. Although exposure therapy may be successful initially, relapse often occurs and is the most prevalent remaining challenge in optimizing treatment efficacy. Research suggests that exposure therapy creates a safety memory that competes for expression with the original threat memory[3,4], suggesting that relapse may occur because of relatively weak learning and retention of the safety memory. Therefore, identifying mechanisms that can be used to strengthen safety learning is a key step in advancing treatment for trauma-related disorders. A promising approach to strengthen safety learning is to create a new, positive association with the event that was previously linked to an aversive outcome. However, while there are indications that establishing positive associations can prevent relapse, the underlying mechanisms are poorly understood (for a review, see [5]).

To study threat responses in a controlled setting, aversive Pavlovian conditioning is typically used. A neutral stimulus (conditioned stimulus, CS; e.g., a picture) is coupled with a biologically aversive unconditioned stimulus (US; e.g., an electrical shock), after which the CS alone also elicits a conditioned threat response. Conditioned threat responses to the CS can be attenuated using extinction, during which the CS is repeatedly presented in absence of the US. However, early theories have suggested that threat responses may more easily be inhibited by engaging appetitive systems[6,7]. Indeed, experiments provide evidence that coupling a CS to a positive US after threat conditioning, a process known as aversive-to-appetitive counterconditioning (CC), may be superior to regular extinction. Specifically, CC compared to regular extinction was associated with a faster attenuation of learned threat responses[6,8], stronger decreases in threat expectancy[9,10], and more positive valence ratings of the CS[11-13] immediately post-CC.

Tests for spontaneous recovery, reinstatement, and renewal can subsequently be used to evaluate the return of threat responses over time, after unsignaled presentation of the US, or in a novel context, respectively[3,14]. Thereby, one can investigate whether CC persistently attenuates threat responses. While early rodent studies showed that CC may be prone to the same relapse as extinction[15,16], recent neurobiological work in rodents showed that CC can enhance the activation of an amygdala-striatal pathway, which is also recruited during extinction – albeit to a lesser degree –, and that CC compared to regular extinction can reduce the return of threat responses[17]. Recent studies suggest that CC may diminish the return of threat responses in humans as well. Specifically, it was shown that CC compared to regular extinction reduced renewal of previously learned food-allergy associations when presented in a novel context one day later[18]. Counterconditioning compared to regular extinction was also associated with reduced recovery of arousal and shock expectancy the following day[9,19], as well as reduced reinstatement[9].

Extinction learning appears to be mediated by activation of the ventromedial prefrontal cortex (vmPFC), which inhibits the expression of threat responses by suppressing amygdala activity[20-23]. When extinction is enhanced by replacing aversive with novel, neutral outcomes, the vmPFC was found to be engaged more effectively than during standard extinction[24]. When extinction is enhanced by replacing aversive outcomes with a reward (counterconditioning), evidence in rodents suggests stronger engagement of the ventral striatum, a region known to be involved in the anticipation and receipt of reward[25]. However, human studies only provide indirect evidence for such

a mechanism since involvement of the ventral striatum could only be shown during spontaneous recovery[19] or during reinstatement[26], but not during CC itself. Although it was observed that brain areas of the fear network are reduced during CC versus regular extinction in humans[19], it is unclear how this difference is achieved. Therefore, although evidence suggests that CC is more effective than regular extinction in preventing the return of threat responses the neural mechanisms are not well understood yet. It remains unclear whether CC is a form of enhanced extinction that is mediated by enhanced engagement of extinction networks, including the vmPFC, or whether it is driven by engagement of reward networks.

To investigate the qualitative differences between CC versus regular extinction further, category conditioning can be used, a procedure in which conditioned threat responses are learnt by coupling a US to conceptually linked exemplars that together form a category (e.g., pictures of animals)[27]. It allows for the typical measures of threat conditioning, but also provides the opportunity to probe episodic memory for the CS category exemplars[28]. When episodic memory was probed 24h after CC and extinction, it was shown that memory for CS+ stimuli that had undergone CC was stronger than memory for CS+ stimuli that had undergone regular extinction[29]. This suggests that compared to regular extinction, CC can enhance episodic memory consolidation and potentially provide stronger retrieval competition against a threat memory.

To investigate the neural mechanisms that distinguish CC from regular extinction and to establish whether CC is indeed associated with a memory that is qualitatively different from the safety memory established during regular extinction, we performed a two-day fMRI study comparing CC versus regular extinction in a between-subjects design (**Figure 1A**). Participants underwent category conditioning and subsequently underwent either aversive-to-appetitive CC (CC group) or regular extinction (Ext group; **Figure 1B-C**). During the CC task, participants in the CC group obtained monetary rewards depending on how quickly they responded to a cue superimposed on novel category exemplars from the CS+ category, a procedure similar to the monetary incentive delay (MID) task[30]. To maximize task similarity between tasks and groups, the cued-response element was kept consistent in all tasks (acquisition, CC/extinction, spontaneous recovery, reinstatement), but response-time contingent monetary rewards were only present during the CC task (**Figure 1F**). To assess the potential of CC versus regular extinction in persistently attenuating the expression of threat response, we tested retrieval of the threat memory and reinstatement of threat responses one day later (**Figure 1D**). Episodic memory for exemplars of the CS categories that were presented during threat conditioning and CC/extinction was assessed by means of a surprise memory test. To characterize pupil dilation responses (PDRs) and skin conductance responses (SCRs) during the anticipation of shock- and reward-reinforcement independently from prior conditioning, a separate valence-specific response characterization task was included at the end of the experiment (**Figure 1E**).

In line with previous results[9,19], we hypothesized that CC compared to extinction would lead to a more persistent attenuation of threat responses. As indicated above, this could be mediated by two possible neural mechanisms: either through enhanced engagement of extinction networks, reflected by increased engagement of the vmPFC, or through a shift towards reward networks, reflected by activation of the ventral striatum. Based on previous results[29], we expected stronger episodic memory for CS exemplars presented during CC, whereas regular extinction would not show such a strengthening effect.

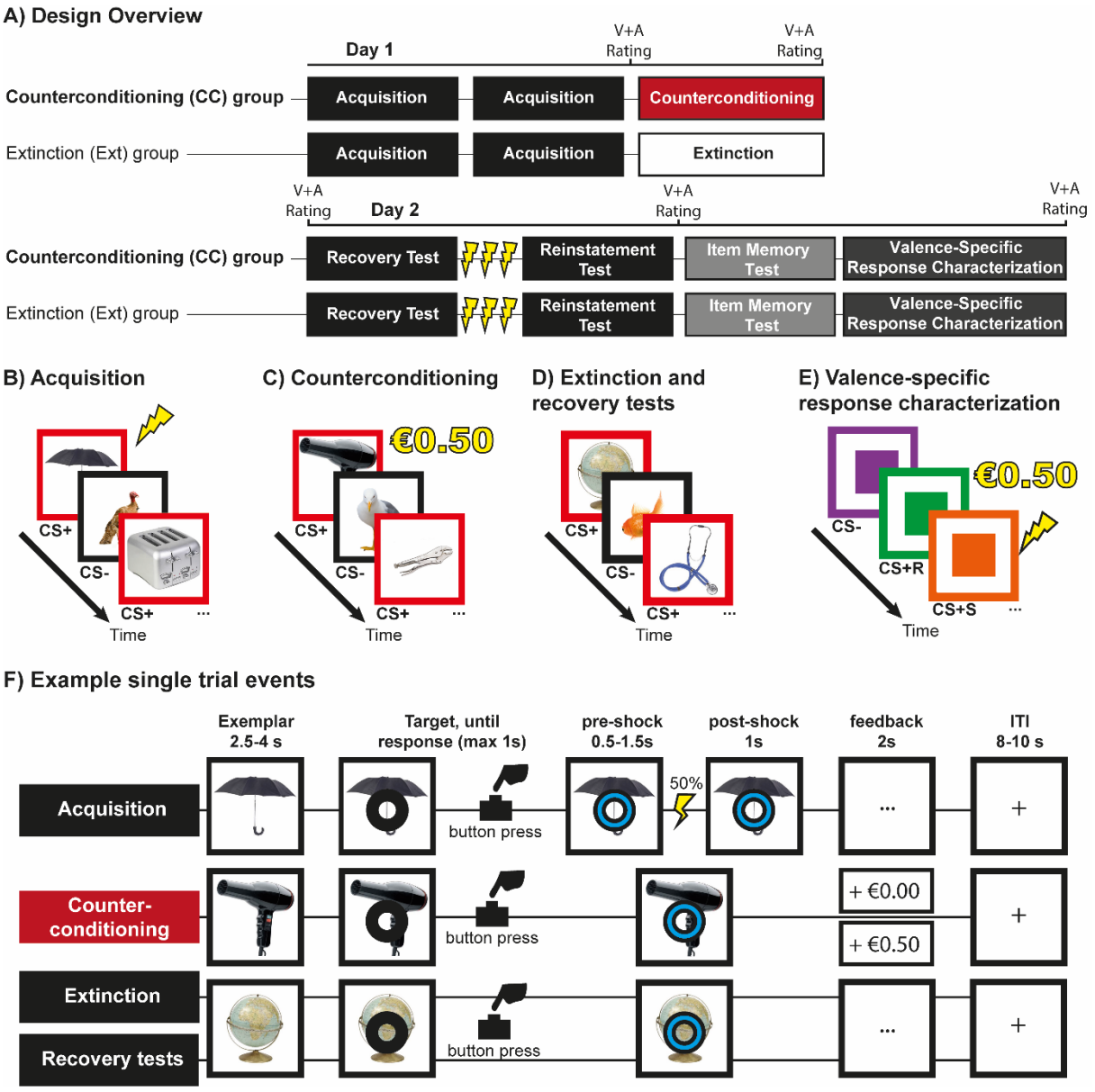

Figure 1. Overview of the experimental design. (A). Participants were assigned to the counterconditioning (CC) or extinction (Ext) group. On day 1, participants performed two blocks of acquisition of category-conditioned threat responses separated by a 30 second break, followed by CC or extinction. Day 2 consisted of a spontaneous recovery test, a reinstatement procedure and test, an item memory test and a valence-specific response characterization. Valence and arousal ratings for the different categories were taken before or after the tasks as indicated by 'V+A Rating'. All tasks were performed in an MRI scanner. **(B)** During acquisition, participants viewed trial-unique exemplars of objects and animals. Exemplars of one category (CS+ animals or objects counterbalanced) were paired with a shock in 50% of trials. CS- trials were not reinforced. **(C)** Participants in the CC group could earn a monetary reward if they responded quickly enough to exemplars in the CS+ category. **(D)** Participants in the Ext group underwent extinction. During the extinction task, recovery test and reinstatement test, neither CS+ nor CS- exemplars were paired with a shock. **(E)** In the valence-specific response characterization task, participants viewed three different coloured squares. One colour was associated with shock (CS+S), one colour with reward (CS+R) and one colour served as CS-. The trial structure was otherwise identical to the acquisition and CC tasks. **(F)** In all Pavlovian tasks, trial onset was marked by presentation of a unique category exemplar. After a variable interval, a ring appeared, to which participants were instructed to respond as quickly as possible. Upon response, the ring shifted in colour as response confirmation. In the acquisition task, shocks could occur 0.5-1.5-seconds after the response window had elapsed (indicated as 'pre-shock). The category exemplar and cue remained visible 1 second after potential shock administration (indicated as 'post-shock'). During CC, participants received visual feedback for 2 seconds (+€0.50 approximately the fastest 70% of trials, +€0.00 on other trials). During the other tasks, participants viewed neutral

feedback (three dots). Trials were separated by an 8-10 s intertrial interval, during which a fixation cross is displayed in the centre of the screen.

Results

In the valence-specific response characterization task, we observed that both threat and reward-anticipation induced strong arousal-related PDRs and SCRs (see **Supplementary Information**). However, PDRs allowed for a better differentiation of the two compared to the CS- (**Supplementary Figure 1A**). Therefore, we focused on PDRs in all analyses and refer to the Supplementary Information for details on the analysis of SCRs. During the acquisition task, both groups showed comparable and successful acquisition of differential conditioned threat responses (PDR means ± SD: CC CS+=1.085±.030, CC CS-=1.054±.033, Ext CS+=1.084±.050, Ext CS-=1.050±.035; for PDR, SCR and fMRI results see **Supplementary Information**).

Extinction and aversive-to-appetitive counterconditioning

After threat acquisition, participants in the CC group underwent CC, while participants in the Ext group underwent regular extinction. Across both groups and phases (early vs. late), we observed retention of conditioned differential PDRs (CS-type (CS+, CS-) x Phase (Early, Late) x Group (CC, Ext) rmANOVA, main effect CS-type: $F_{(1,34)}=15.393$, $p<0.001$, $\eta^2=0.312$, **Figure 2A**), as well as a decrease in PDRs over the course of the task (main effect phase: $F_{(1,34)}=10.121$, $p=0.003$, $\eta^2=0.229$). These findings are in contrast to our expectation of a CS-type x Phase x Group interaction. Specifically, we expected differential PDRs to become extinguished in the Ext group, while being sustained in the CC group, potentially due to increased reward anticipation. Extinction in the Ext group however already occurred during the early phase (paired t-test, early CS+ vs. CS-, p=0.233), and differential responses did not change towards the late phase (p=0.979). As a result, we found distinct differential conditioned PDRs throughout the CC/extinction task between groups (CS-type x Group interaction: $F_{(1,34)}=6.053$, $p=0.019$, $\eta^2=0.151$), with participants undergoing CC showing stronger PDRs to CS+ vs. CS- category exemplars (paired t-test average CS+ vs. CS-, t(20)=3.602, p=0.002, CS+: 1.07±0.04, CS-: 1.04±0.04), whereas differential PDRs were extinguished in participants undergoing extinction (paired t-test average CS+ vs. CS-, p=0.246, CS+: 1.05±0.04, CS-: 1.04±0.04). Results of the valence-specific response characterization task showed that differential PDRs can also be indicative of anticipation of reward (**Supplementary Figure 1A**). Thus, while PDRs in the Ext group indicated that differential conditioned threat responses were successfully extinguished, differential PDRs persisted in the CC group, likely reflecting reward anticipation. Differential SCRs persisted during the late phase

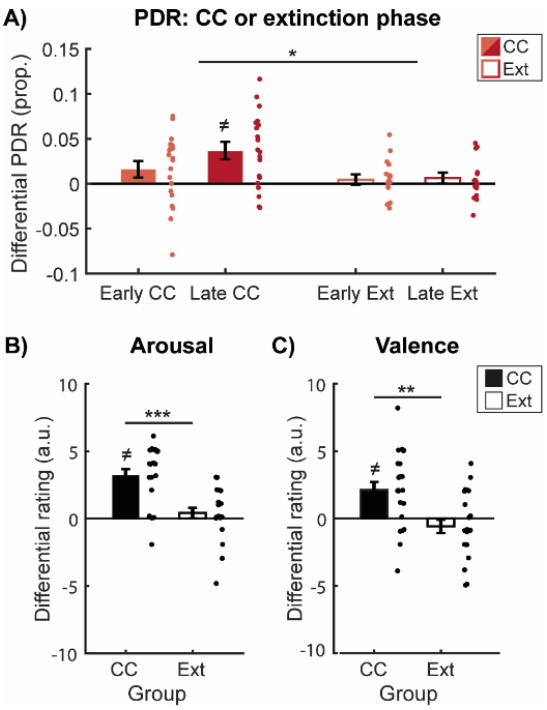

Figure 2. Differential PDRs during CC/extinction and explicit ratings of arousal and valence provided after the counterconditioning or extinction phase. (A) Differential PDRs for the early (light red) and late (dark red) phase of counterconditioning (CC, solid bars) or extinction (EXT, open bars). Participants undergoing CC showed increased differential PDRs as compared to participants undergoing extinction. (B) Arousal and (C) valence ratings displayed separately for participants assigned to the counterconditioning (CC, solid bars) and extinction (EXT, open bars) groups. Participants that had undergone CC gave stronger differential arousal scorings than participants that had undergone extinction. In addition, participants that underwent CC showed flipped differential valence ratings: while valence differential valence ratings were negative after extinction, the direction reversed to positive differential ratings after CC. Error bars represent ± standard error of the mean. *=p<0.05, **=p<0.01, ***=p<0.001, ≠ indicates that the bar is significantly different from 0.

of both CC and extinction but were no longer detectable in the last two trials and were comparable between groups (see **Supplementary Information**).

Valence and arousal ratings provide further support for the extinction of differential responses in the Ext group and positive, reward-induced arousal for CS+ items in the CC group (**Figure 2B-C**). Differential valence ratings for the CS+ and CS- differed between groups after the CC/extinction task (CS-type (CS+, CS-) x Group (CC, Ext) rmANOVA, CS-type x Group interaction: $F(_{1,44})=12.054$, $p=0.001$, $\eta^2=0.215$). Participants in the CC group rated CS+ stimuli more positive than CS- stimuli ($t(21)=3.469$, $p=0.002$, CS+: 7.5±0.30, CS-: 5.41±0.38), while participants in the Ext group gave both categories similar valence ratings ($p=0.245$, CS+: 5.63±0.32, CS-: 6.21±0.28). Differential arousal ratings for the CS+ and CS- also differed between groups (CS-type (CS+, CS-) x Group (CC, Ext) rmANOVA, CS-type x group interaction: ($F(_{1,44})=20.862$, $p<0.001$, $\eta^2=0.322$). Participants in the CC group reported higher arousal levels for the CS+ category than for the CS- category ($t(21)=6.370$, $p<0.001$, CS+: 6.64±0.20, CS-: 3.45±0.38) while participants in the Ext group gave similar arousal ratings for the CS+ and CS- categories ($p=0.290$, CS+: 4.21±0.43, CS-: 3.80±0.40). Taken together, more positive valence and higher arousal ratings for the CS+ in the CC group as compared to the Ext group further support the interpretation of increased differential PDRs reflecting arousal induced by reward anticipation.

CC prevents differential spontaneous recovery

To investigate whether CC prevented the spontaneous recovery of differential conditioned threat responses, we compared PDRs in the last two trials of the CC/extinction phase and the first two trials of the spontaneous recovery test in a CS-type (CS+, CS-) x Group (CC, Ext) x Phase (last two trials of CC/extinction, first two trials of the spontaneous recovery test) rmANOVA. We expected the Ext group to show an increase in PDRs from the extinction task to the spontaneous recovery task, while we expected PDRs for the CC group to remain stable or decrease. Critically, differential spontaneous recovery of PDRs differed between groups (Group x CS-type x Phase interaction: $F(_{1,28})=6.329$, $p<0.018$, $\eta^2=0.184$, **Figure 3**). While the CC group showed a decrease in differential PDRs from CC to spontaneous recovery ($t(14)=-1.807$, $p=0.046$, one-tailed, CC: 0.34±0.2, spontaneous recovery: -0.01±0.18), the Ext group showed an increase in differential PDRs ($t(14)=1.850$, $p=0.043$, one-tailed significance, extinction: 0.11±0.01, spontaneous recovery: 0.04±0.02). To conclude, while we observed differential spontaneous recovery in the Ext group, we did not find evidence for differential spontaneous recovery in the CC group, suggesting that CC attenuated the recovery of threat-responses compared to regular extinction.

However, since participants undergoing CC showed persistent differential PDRs during the last two trials of the CC phase, while participants undergoing extinction did not, we additionally explored whether there was differential responding during the first two trials of the spontaneous recovery test. During the first two trials of the spontaneous recovery test, participants in the CC group showed decreased differential PDRs as compared to the Ext group (CS-type (CS+, CS-) x Group (CC, Ext) rmANOVA, CS-type x Group interaction: $F(_{1,29})=3.901$, $p=0.029$, one-tailed, $\eta^2=0.119$). Further exploration within the groups confirmed that participants in the CC group did not show retention of differential responses (paired t-test, CS+ and CS- responses during the first two trials of the spontaneous recovery test, $p=0.219$, one-tailed), while the Ext group did show increased responses to the CS+ as compared to the CS- ($t(14)=1.958$, $p=0.035$, one-tailed). Thus, both the differential spontaneous recovery of PDRs between sessions, and differential responding within the first two trials of the spontaneous recovery test suggested that CC prevented spontaneous recovery of differential responses compared to extinction. SCRs did not show differential recovery and were comparable between groups (see **Supplementary Information**).

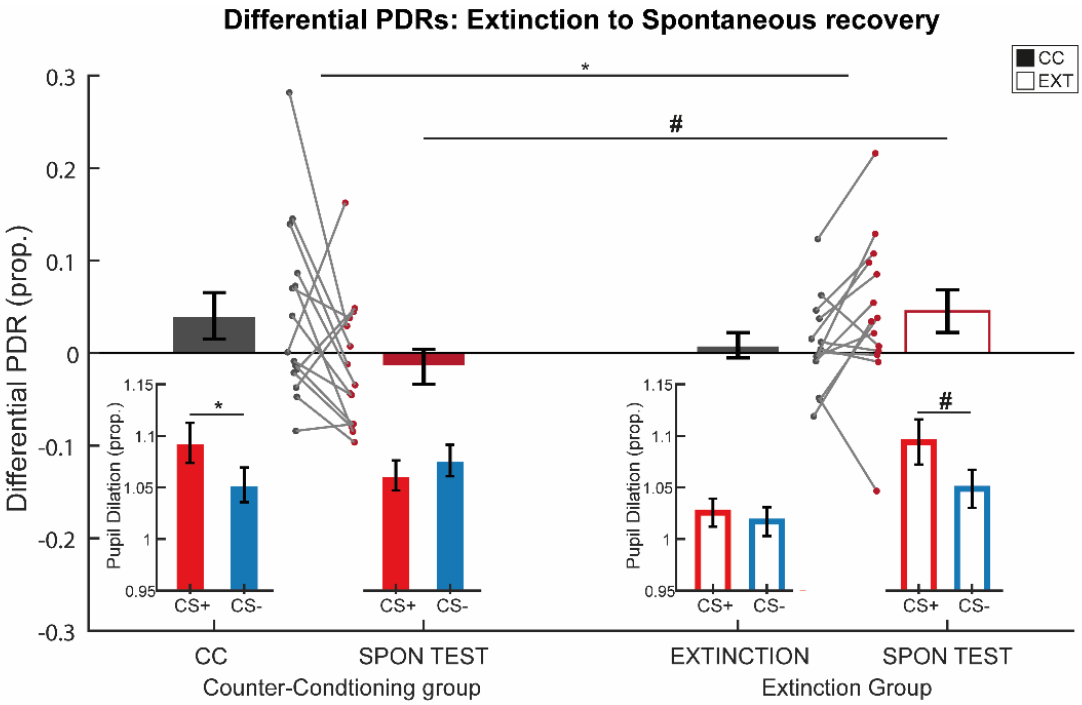

Figure 3. Differential PDRs during the last two trials of extinction (grey) and the first two trials of the spontaneous recovery test (dark red). Differential PDRs show selective spontaneous recovery after extinction (Ext group, open bars) but not after CC (CC group, solid bars). During the first two trials of the spontaneous recovery test, differential PDRs are increased in the Ext group as compared to the CC group. Insets show PDRs to the CS+ (red) and CS- (blue) during the last two trials of extinction and the first two trials of the spontaneous recovery test. While the Ext group shows differential responding during the spontaneous recovery test, the CC group does not. Error bars represent ± standard error of the mean. *=p<0.05, #=p<0.05 one-tailed significance.

CC also appeared to have lasting beneficial effects on valence ratings compared to extinction. At the start of the second testing day, differential valence ratings continued to differ between groups (CS-type (CS+, CS-) x Group (CC, Ext) rmANOVA, CS-type x Group interaction: $F_{(1,44)}$=5.160, p=0.028, η^2=0.105). While participants in the CC group gave similar valence ratings to both categories (p=0.179, CS+: 6.3±0.34, CS-: 5.4±0.35), participants in the Ext group gave more negative valence ratings to the CS+ category than to the CS- category (t(23)=-1.964, p=0.031 one-tailed test, CS+: 5.5±0.30, CS-: 6.3±0.24), also illustrative of relapse of threat associations.

Surprisingly, while participants in the CC group showed heightened differential arousal ratings immediately after CC as compared to ratings from participants who had undergone extinction (**Figure 2B**), participants in both groups gave comparable differential arousal ratings at the start of the second day immediately before the spontaneous recovery test (CS-type (CS+, CS-) x Group (CC, Ext) rmANOVA, main effect of CS-type: $F_{(1,44)}$=10.932, p=0.002, η^2=0.022, CS+: 4.8±0.28, CS-: 3.9±0.24). Likewise, response times to the CS+ and CS- during the first two trials of the spontaneous recovery task were similar across both groups (all p's>0.2). These findings may suggest that differential arousal evoked by the categories was similar in both groups immediately before and during the spontaneous recovery test.

The spontaneous recovery test was followed by a reinstatement procedure, consisting of three unsignaled shocks, and a reinstatement test. However, mean PDRs decreased from spontaneous recovery to reinstatement (t(30)=3.063, p=0.005, last two trials of spontaneous recovery: 1.04±0.01, first two trials of reinstatement: 1.01±0.01). Given that we did not observe successful reinstatement in either group, our reinstatement test was not informative on whether CC can lead to a more

258 persistent attenuation of threat responses as compared to regular extinction. A full description of
259 PDR and SCR results of the reinstatement test can be found in the **Supplementary Information**.

260 Distinct CS-type specific activation for extinction and appetitive counterconditioning

261 After acquisition, the CC group underwent appetitive CC, while the Ext group underwent regular
262 extinction. Whole brain analysis revealed that over the course of this task, CS-type specific activation
263 changed differentially between the two groups in a large cluster encompassing multiple regions in
264 the medial temporal lobe (Group x CS-type x Phase interaction, cluster size = 1760 mm^3, p=0.034,
265 whole-brain FWE-corrected, **Figure 4B** and **Table 1**). We further investigated the anatomical location
266 of the cluster using our ROIs to probe for activity and found that the effect encompassed the
267 amygdala. To further investigate the interaction effect in the amygdala, we extracted parameter
268 estimates from the complete bilateral amygdalae (Automated Anatomic Labelling, AAL, atlas in the
269 WFU PickAtlas toolbox in MN152 space) and performed post-hoc comparisons. In the early phase,
270 CS-type specific responses differed between the groups (t(1,44)=2.173, p=0.035, CC: 0.18±0.08, Ext: -
271 0.073±0.08). Specifically, the CC group showed increased amygdala activation to the CS+ as
272 compared to the CS- (t(23)=2.210, p=0.037) while that was not the case in the Ext group (p=0.390). In
273 the late phase, differential responses were comparable between the groups (p=0.503).

274 Whole-brain analysis further revealed a number of clusters showing distinct CS-specific activations
275 between groups throughout the task, including the anterior cingulate, cuneus, nucleus accumbens,
276 caudate, thalamus and inferior frontal gyrus (**Figure 4A**, **Table 1**). The group and stimulus-specific
277 activation of the NAcc was in line with a priori expectations for the CC phase (**Figure 4C**). To further
278 explore this effect, averaged parameter estimates from the bilateral NAcc ROI (mask acquired from
279 the IBASPM 71 atlas in the WFU PickAtlas toolbox in MNI152 space) were extracted. Across the
280 bilateral NAcc, differential activation was increased in the CC as compared to the Ext group
281 (t(44)=2.731, p=0.009, CC: 0.37±0.10, Ext: 0.04±0.06), with the CC showing increased NAcc activation
282 to the CS+ compared to the CS- (t(23)=6.194, p<0.001, CS+: 0.59±1.12, CS-: 0.16±0.09) whereas the
283 Ext group did not (p=0.574).

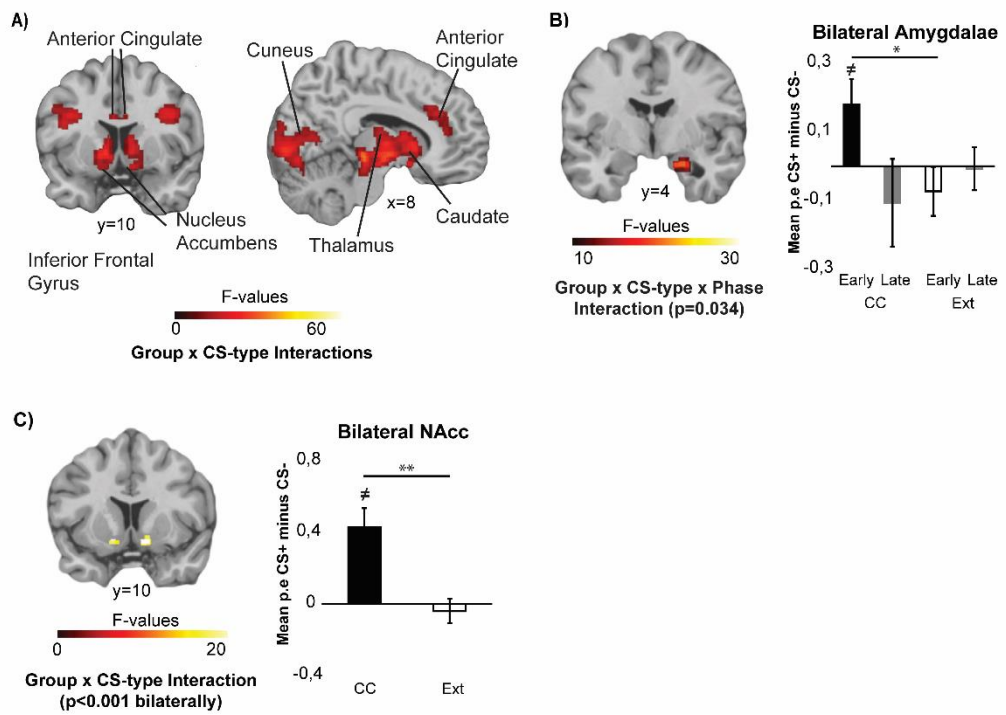

Figure 4. Stimulus-type specific activation differs between participants undergoing CC versus extinction. A. Whole-brain Group x CS-type interaction effects revealed distinct stimulus-specific activation of regions including the anterior cingulate, cuneus, nucleus accumbens, caudate, thalamus and inferior frontal gyrus during the counterconditioning vs. extinction phase. Panel A displays group F-images (see **Table 1** for directions) FWE-corrected at p<0.05, cluster-forming threshold p=0.001. **B**. The right amygdala showed a Group x CS-type x Phase interaction during the CC/extinction task, indicating that CC compared to extinction is associated with decreased activation of the amygdala**. C.** The bilateral NAcc showed a Group x CS-type interaction during the CC/extinction task, revealing increased NAcc activation in response to the CS+ compared to the CS- in the CC but not in the Ext group. Panel B and C display group F-images FWE-SVC at p<0.05, cluster-forming threshold p=0.001, along with post-hoc tests on mean parameter estimates from the complete ROI included in the analyses. ** p<0.01, * p<0.05, ≠ indicates that the value is significantly different from 0.

Table 1. Whole-brain main effects of group (CC, Ext), CS type (CS+, CS-) and phase (early, late) and interactions, during the counterconditioning/extinction task. Cluster-forming threshold p=0.001, FWE-corrected at p<0.05, clusters were labelled using the Talairach Daemon atlas and the AAL atlas for ROIs. For each cluster, the peak voxel coordinates (MNI space) and regions are reported, and additional regions contained within the cluster are added in italics. See **Supplementary Table 1** for main effects of CS-type.

		Peak MNI coordinate						
Region	***Cluster***	***x***	***y***	***z***	***Size (mm3)***	***pFWE (cluster)***	***Peak F-value***	***Direction***
Group x CS-type x phase								
Parahippocampal Gyrus BA34R *Parahippocampal Gyrus Amygdala, Uncus BA34R*	1	18	-8	-20	1760	0.034	23.40	CS+>CS- difference increases from early to late phase for CC, not for Ext
Group x CS-type								
Lateral Geniculum Body LR, Caudate Head LR, Thalamus LR, Lentiform Nucleus LR	1	2	-26	-18	29920	<0.001	73.15	(CC CS+>CS-) > (Ext CS+>CS-)
Cuneus L *Lingual Gyrus BA17/BA18 LR, Posterior Cingulate LR, Cuneus BA18R, Cuneus BA30L Declive R*	2	-6	-96	2	23272	<0.001	43.50	
Inferior Frontal Gyrus BA47L *Insula BA13 L*	3	-36	18	-6	4504	0.009	30.62	
Extra-Nucleus R	4	30	26	2	3136	0.016	37.67	
Superior Temporal Gyrus L *Superior Temporal Gyrus BA41 L, Transverse Temporal Gyrus L*	5	-60	-44	14	9088	0.002	43.56	
Transverse Temporal Gyrus BA41 R *Superior Temporal Gyrus R, Superior Temporal Gyrus BA42/BA22R*	6	44	-22	12	7784	0.003	42.17	
Anterior Cingulate BA32R *Anterior Cingulate BA32L, Cingulate Gyrus R*	7	6	30	26	8880	0.002	27.90	
Precentral Gyrus L *Inferior Frontal Gyrus L*	8	-36	0	30	3624	0.014	30.10	
Precentral Gyrus R *Sub-Gyral R*	9	40	2	32	4056	0.011	40.64	
Precentral Gyrus BA6L *Middle Frontal Gyrus BA6L*	10	-44	-6	52	2184	0.028	24.34	(CC CS+>CS-) > (Ext CS+>CS-)
Angular Gyrus R *Supramarginal Gyrus R*	11	54	-60	36	1944	0.032	24.18	
Group x Phase								
No significant clusters								
CS-type x Phase								
No significant clusters								
Group								
No significant clusters								
Phase								
Inferior Frontal Gyrus R *Inferior Frontal Gyrus BA45 R*	1	30	26	8	4848	0.006	40.27	Early Phase > Late Phase
Insula L *Superior Temporal Gyrus BA22, Precentral Gyrus L*	2	-28	26	0	4368	0.007	38.41	
Postcentral Gyrus L	3	-54	-24	22	1768	0.031	23.75	

Contrast estimates in further a priori defined ROIs during the CC/Ext task were submitted to a Group (CC, Ext) x CS-type (CS+, CS-) x Phase (early, late) rmANOVA (**Figure 5**). The bilateral hippocampi (right hippocampus cluster size: 664 mm^3, p=0.001, FWE-SVC, left hippocampus cluster size: 112 mm^3,

p=0.024, FWE-SVC) and the left vmPFC (mask defined as bilateral gyrus rectus and medial orbital gyri, cluster size = 160 mm^3, p=0.013, FWE-SVC) showed differentially changing CS-type-specific activations between the groups (Group x CS-type x Phase interaction). While CS+-specific suppression of these regions appeared to increase during the CC task, this was not the case during the extinction task. Post-hoc comparisons on averaged parameter estimates in the bilateral hippocampi confirmed that stimulus-specific suppression increased during the course of the task in the CC group (t(23)=3.280, p=0.003, early CS+-CS-: 0.054±0.07, late: -0.150±0.07), but not in the Ext group (p=0.266). Post-hoc comparisons across the vmPFC ROI also revealed increased CS+-specific suppression in the CC group compared to the Ext group (t(44)=2.221, p=0.032, CC: -0.189±0.06, Ext: -0.070±0.10). While the extinction group showed increased CS+-specific activation from the early to the late phase of the extinction task (t(21)=2.235, p=0.036, early CS+: -0.149±0.08, late CS+: 0.040±0.09), the CC group did not (p=0.120). During the late phase, the CC group showed increased vmPFC deactivation to the CS+ compared to the CS- (t(23)=3.174, p=0.004, late CS+: -0.284±0.06, late CS-: -0.095±0.05), while the Ext group did not (p=0.503). Thus, across both the hippocampus and the vmPFC, CC induced increased stimulus-specific suppression.

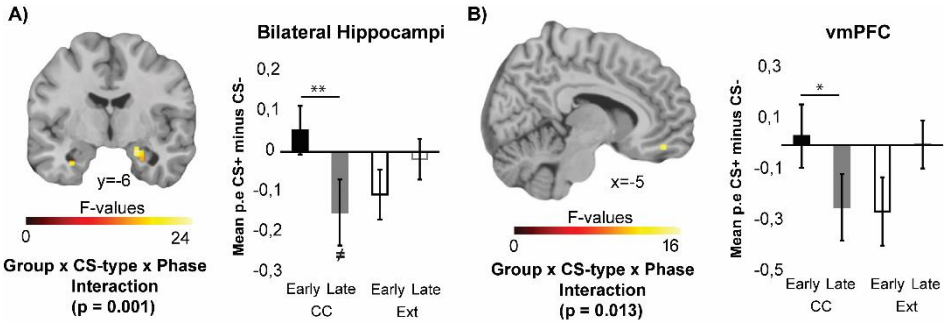

Figure 5. ROI analyses during the CC/extinction task reveal distinct activity in the hippocampus and left vmPFC. During the CC/extinction task, stimulus-specific activation of the hippocampus (C) and left vmPFC (**D**) changes differently between groups. ** p<0.01, * p<0.05, ≠ indicates that the bar is significantly different from 0. Group F-images FWE-SVC at p<0.05, cluster-forming threshold p=0.001, along with post-hoc tests on mean parameter estimates from complete ROI included in the analyses.

During the spontaneous recovery task, a priori defined regions of interest did not reveal any effects (see **Supplementary Information**).

Counterconditioning retroactively enhances item recognition for conditioned exemplars

Following the reinstatement test and re-extinction, participants completed a surprise item recognition test approximately 24 hours after acquisition and the CC/extinction task. One outlier was excluded from this analysis (CS- false alarm rate = 0.91). Threat conditioning has previously been shown to enhance 24-hour item recognition for category exemplars presented during the acquisition phase[27]. However, this enhancement for CS+ items did not extend to items presented during an extinction session separated from the acquisition phase by a short break[31]. We therefore analysed item recognition for the CS+ and CS- during acquisition and the CC/extinction phase separately to examine whether the groups differed in recognition memory performance (**Figure 6**).

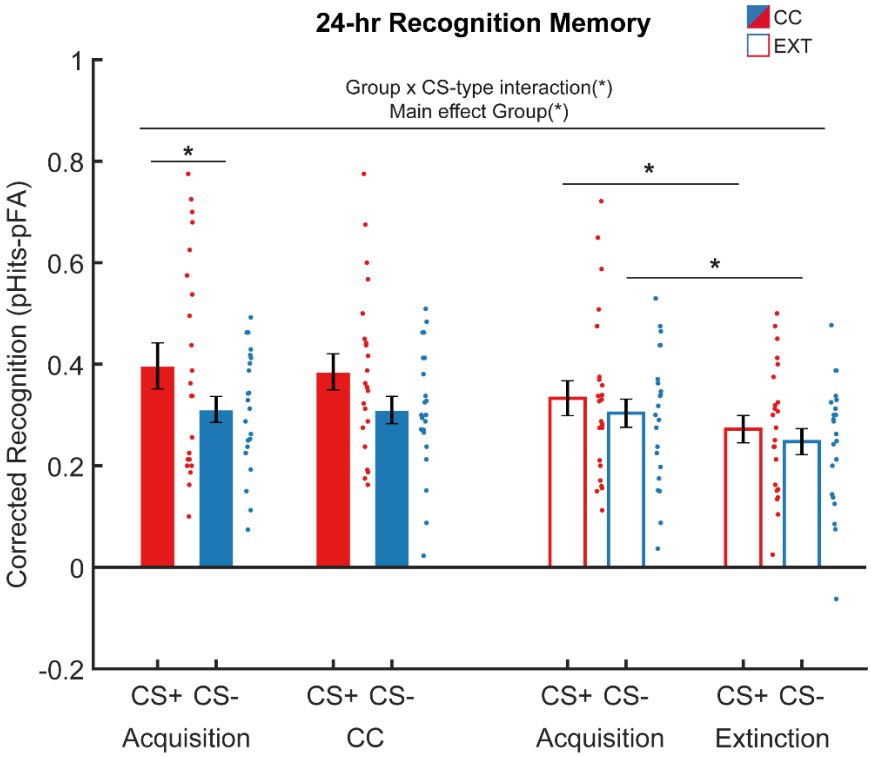

Figure 6. Twenty-four hour recognition memory results. During acquisition and extinction on the first day of the experiment, participants viewed trial-unique exemplars from two semantic categories (objects, animals) that served as CS+ and CS-. The next day, participants completed a surprise memory test for these items, mixed with an equal number of novel exemplars. Participants recognized relatively more items from the CS+ category, and participants that underwent CC showed improved item recognition compared to participants in the Ext group. Error bars represent ± standard error of the mean. *=p<0.05.

Corrected recognition scores (hits probability-false alarms probability) were subjected to a task (acquisition, CC/extinction task) x CS-type (CS+, CS-) x Group (CC, Ext) rmANOVA, including CS+-category (animals, tools) as covariate. Overall, participants showed better memory for items from the CS+ category (main effect of CS-type: ($F_{(1,42)}$=10.615, p=0.002, η^2=0.202) and participants who underwent CC showed better memory as compared to participants who underwent extinction (main effect of Group: ($F_{(1,42)}$=4.963, p=0.031, η^2=0.106). Stimulus-type specific item recognition differed between the CC and Ext groups (CS-type x Group interaction: $F_{(1,42)}$=4.535, p=0.039, η^2=0.094). While participants in the CC group showed better recognition memory for the CS+ category compared to the CS- category (t(22)=2.531, p=0.019, means ± SD: CS+ 0.39±0.17, CS- 0.31±0.10), this was not the case for participants in the Ext group (t(23)=0.889, p=0.384, means ± SD: CS+ 0.30±0.13, CS- 0.28±0.11). Although the effect of stimulus-type was stronger for tools as CS+, this was not different between groups (see **Supplementary Information**). Thus, across the acquisition and CC/extinction phase, participants who underwent CC showed a stronger enhancement of CS+ memory compared to the participants that underwent extinction.

To further investigate to what extent CC retroactively affected memory for items presented during the acquisition task, we examined item recognition during acquisition and the CC/extinction tasks separately. While threat conditioning increased memory for CS+ items presented during the acquisition task across both groups (main effect CS-type: ($F_{(1,42)}$=18.147, p=<0.001, η^2=0.302), subsequent CC enhanced this effect (Group x CS-type interaction: ($F_{(1,42)}$=5.112, p=0.029, η^2=0.109). Post-hoc tests revealed increased item memory for the CS+ category compared to the CS- category presented during acquisition in the CC group (t(22)=2.341, p=0.029, means ± SD: CS+ 0.40±0.21, CS- 0.31±0.12) but not in the Ext group (t(23)=0.818, p=0.422, means ± SD: CS+ 0.33±0.16, CS-

366 0.30±0.13). Again, although the effect of stimulus-type was stronger for tools as CS+, this was not
367 different between groups (see **Supplementary Information**). As the acquisition task was identical
368 between groups, it appears that CC in comparison to extinction retroactively enhanced memory for
369 CS+ items. For items presented during the CC/extinction task, overall item recognition was better in
370 the CC group compared to the Ext group (main effect group: $F(_{1,42})=8.706$, $p=0.005$, $\eta^2=0.172$, means
371 ± SD: CC 0.35±0.12, Ext 0.26±0.09). Thus, compared to regular extinction, CC enhanced recognition of
372 items presented during CC, but interestingly also strengthened the emotional memory enhancement
373 of CS+ exemplars presented during acquisition, suggesting that immediate CC may alter consolidation
374 of a prior threat learning episode.

375 Following previous work[29,31,32], we explored stimulus-type specific decreases in item recognition
376 between tasks, as well as within-phase differences between item recognition for the CS+ and CS-
377 within each group. As expected, a post-hoc paired samples t-test showed that participants in the Ext
378 group remembered significantly more CS+ items from the acquisition phase as compared to the
379 extinction phase ($t(23)=2.238$, $p=0.036$, means ± SD: acquisition 0.33±0.16, extinction 0.27±0.13). In
380 contrast, participants who had undergone CC remembered CS+ items presented during acquisition
381 and CC equally well ($t(22)=0.390$, $p=0.701$, means ± SD: acquisition 0.40±0.21, CC 0.38±0.16). Thus,
382 while recognition memory for items encoded during the extinction task was substantially weaker
383 than memory for items from the acquisition task, this was not the case for items presented during
384 CC.

385 Discussion

386 This study aimed to test whether CC compared to regular extinction can lead to a more persistent
387 attenuation of threat responses, and to investigate whether this is mediated by neural mechanisms
388 reflecting extinction-related enhanced engagement of the vmPFC or engagement of reward-focused
389 networks. We found that CC prevented differential spontaneous recovery of PDRs compared to
390 regular extinction, suggesting that CC reduces the recovery of threat responses. Our fMRI results
391 suggested that CC engages different neural mechanisms compared to extinction. Most notably, while
392 the extinction group showed an increase in CS+-specific vmPFC activation during extinction, the CC
393 group showed CS+-specific deactivation of the vmPFC that persisted throughout the late phase of CC.
394 Furthermore, CC led to increased NAcc activation for the CS+ compared to the CS-, whereas this was
395 not the case for extinction. Lastly, phase- and stimulus-specific activation of the hippocampus and
396 the amygdala differed between extinction and CC. Compared to extinction, CC led to increased
397 activation of the amygdala in the early phase, and increasing stimulus-specific deactivation of the
398 hippocampus over the course of the early and late phases. In addition, CC retroactively enhanced
399 item recognition for conditioned exemplars presented during acquisition and strengthened memory
400 for conditioned exemplars presented during CC compared to extinction.

401 The mechanism underlying CC appears to be qualitatively different from the mechanism underlying
402 regular extinction. Regular extinction is associated with activation of the vmPFC[23,33], which is thought
403 to inhibit the expression of threat responses by suppressing amygdala activity[20-23]. In comparison to
404 regular extinction, novelty facilitated extinction, a form of enhanced extinction, in which aversive
405 events are replaced with novel neutral outcomes, has shown stronger CS+-specific vmPFC
406 activation[24]. If CC was similarly mediated by enhanced recruitment of extinction networks, we would
407 have expected increased activation of the vmPFC, yet we observed a CS+-specific deactivation of the
408 vmPFC during CC, disproving this hypothesis. Interestingly, deactivation of the vmPFC during CC was
409 also found in studies investigating a form of counterconditioning induced by means of real-time fMRI
410 decoded neurofeedback[34,35]. During neurofeedback CC, participants implicitly learned to obtain
411 monetary rewards by generating a representation of the target CS+ in the visual cortex[34]. After

412 neurofeedback CC, reductions in threat responses were stronger in participants showing stronger
413 vmPFC deactivation, suggesting that vmPFC disengagement may be associated with fear reductions[34].
414 Taken together, both our findings and previous neurofeedback studies suggest that in contrast to
415 enhanced extinction, CC disengages the vmPFC. Given that we replicate this finding using a different
416 approach that includes direct exposure to the CS+, vmPFC disengagement may be a distinguishing
417 characteristic of CC. The observed pattern of activity, including vmPFC deactivation further bears
418 resemblance to activity patterns observed during goal-directed eye movements in an experimental
419 model of eye-movement desensitization and reprocessing (EMDR), which has also been shown to
420 improve extinction learning[36]. A similar activity pattern and effect has also been found for working
421 memory-like tasks, such as a game of Tetris[37-39]. Given that the above-mentioned tasks associated
422 with vmPFC deactivation share their strong engagement of working memory and/or endogenous
423 attention mechanisms, thereby engaging the executive control-network, deactivation of the vmPFC
424 and hippocampus could be the result of a deactivated default mode network due to competition
425 between activation of large scale brain networks[40-42].

426 The CC procedure led to clear CS+-specific activation of the NAcc, which is in line with expectations
427 for reward anticipation in tasks with a monetary incentive delay aspect[43]. Activation of the ventral
428 striatum has also been reported for active avoidance, and may be generally associated with
429 instrumental actions as opposed to passive delivery of an outcome[44,45]. In line with studies on active
430 avoidance, delivery of a reward contingent on instrumental actions has been shown to yield CC that
431 is more resistant to renewal[46]. CS+-specific activation of the NAcc was not seen in participants
432 undergoing extinction, suggesting that this activation is specific to CC. However, previous work in
433 rodents revealed an amygdala-ventral striatum (NAcc) pathway that is activated during extinction
434 training[17]. The recruitment of this pathway was shown to be enhanced during CC, and reduced the
435 return of fear[17], suggesting that CC may in fact enhance activation of reward-related networks that
436 are weakly activated by extinction. Indeed, fMRI studies in humans that modelled prediction error for
437 omitted aversive outcomes during extinction training (i.e. outcomes "better-than-expected") showed
438 involvement of the NAcc[47-49]. Possibly, activation of the NAcc during extinction is limited to early
439 extinction trials generating prediction errors. Nevertheless, based on our findings, it appears that
440 sustained CS+-specific activation of the NAcc is a distinct mechanism underlying CC but not
441 extinction, which is potentially associated with instrumental actions.

442 A recent neuroimaging study suggests that the neural differences between regular extinction and CC
443 may be maintained over time[19]. In their within-subject study, two CS+ categories (animals, objects)
444 were used during threat conditioning. Subsequently one of the CS+ categories was used for regular
445 extinction, whereas the other was used for CC. During CC, CS+ exemplars were paired with positively
446 valenced pictures. During a spontaneous recovery task the following day, it was shown that
447 involvement of the vmPFC (amygdala-vmPFC functional connectivity) was stronger for regular
448 extinction compared to CC. In contrast, CS+-specific increases in functional connectivity between the
449 amygdala and the ventral striatum (NAcc) were only observed in the CC condition during a
450 spontaneous recovery task. Both findings are in line with the CC-associated vmPFC deactivation and
451 NAcc activation that we observed and suggest that differences in the neural mechanisms of regular
452 extinction and CC may be maintained during threat retrieval.

453 CC compared to regular extinction also strengthened item memory for the conditioned category.
454 While both reward and threat conditioning can enhance item recognition for the CS+ category[27,50],
455 recognition of CS+ exemplars presented during extinction was shown to drop compared to
456 acquisition[31]. In contrast to extinction, within-session CC was previously shown to enhance memory,
457 suggesting that CC has a unique, strengthening effect on memory[29]. In the current study, we replicate

this finding, showing strengthened memory after CC compared to extinction. While enhanced recognition of items presented during CC could be mediated by attentional prioritization[51], CC also retrospectively strengthened memory for items presented during acquisition, suggesting that CC may alter the consolidation of a prior threat conditioning episode. Retroactive enhancement of memory consolidation for related items has previously been shown for conceptually related neutral items presented prior to threat conditioning[32] and reward conditioning[50]. At a neurobiological level, these findings have been related to the synaptic tagging-and-capture hypothesis postulating that memories for neutral events can be strengthened if they are followed by salient events, due to an initially short-lived synaptic "tag" that allows later events to stabilize the memory[32,52,53]. At a systems level, retroactive memory strengthening has been linked to reverse replay[54]. Specifically, animal research indicates that rewards increase reverse replay[55-57], and reward-induced reverse replay occurs concurrently with firing of midbrain dopamine neurons[58]. Interestingly, spontaneous replay is also involved in regular extinction, in which unexpected omission of the US drives spontaneous reactivation of activity patterns in the vmPFC. This spontaneous reactivation was shown to be predictive of extinction recall and could be amplified through pharmacological enhancement of dopaminergic activity[59]. Yet while physiological dopaminergic modulation during extinction may be limited to prediction error signals during the early phase[47-49], dopaminergic modulation may be sustained throughout the MID-based CC task applied in this study. While we did not measure dopaminergic activity directly, activation of the NAcc during reward anticipation is predictive of dopamine release within the NAcc[60-63]. Given the increased stimulus-specific activation of the NAcc in the CC group, it is likely that dopaminergic activity was enhanced during CC compared to regular extinction. The enhanced dopaminergic modulation could strengthen memories through replay[55,64], or may increase synaptic plasticity directly, potentially explaining enhanced item recognition after CC compared to regular extinction[54,65,66]. In line with these findings, research in humans shows that reward systematically modulates memory for neutral objects in a retroactive manner, with objects closest to the reward being prioritized[54]. It could be that reward-conditioning during CC similarly drives reward-driven reverse replay, enhancing episodic memory for conceptually related items presented during the preceding acquisition task.

Several limitations of the current study are worth considering. First, while the monetary incentive aspect during CC clearly induced positive valence, it also increased physiological arousal, making it difficult to isolate the individual effects of positive valence and reward-induced arousal. While the current results are in line with previous work in CC using low-arousal, positive-valence pictures[29], we cannot exclude the possibility that the current findings (in part) reflect differences in task engagement between participants due to active instead of passive reward delivery. However, it is questionable whether it is meaningful to tease individual effects of valence and arousal apart since arousal may facilitate reward processing. Indeed, striatal responses to obtained monetary rewards are dependent on salience and are increased when rewards are dependent on active responses compared to passive delivery[67]. Second, although we included a reinstatement procedure in the experiment, neither the Ext nor the CC group showed differential reinstatement. It is worth noting however that reinstatement paradigms in humans may not reliably produce differential reinstatement after extinction[68]. Third, it is important to note that CC/extinction was carried out within minutes after the acquisition phase, and the effects of CC and extinction may differ when carried out after the acquisition memory has been consolidated [69-72]. Fourth, whole-brain analysis of the CS-specific activation during the spontaneous recovery test in the Ext group did not yield any clusters above threshold, while physiological results indicated spontaneous recovery of differential threat responses. Given that recovered threat responses are often quick to extinguish and fMRI

analyses require averaging across multiple trials to achieve sufficient signal-to-noise ratio, threat-evoked neural activity may have been too brief to be detected.

In conclusion, our findings show that appetitive CC improves the retention of safety memory over standard extinction. Strikingly, in contrast to activation of the vmPFC during extinction, CC was associated with stimulus-specific deactivation of the vmPFC. These findings may inform development of future treatments for fear- and anxiety disorders. While a large body of research focuses on enhancing regular extinction, this study indicates that another promising and potentially longer-lasting approach may be to engage reward-circuits. Although further work is needed, a major advantage of CC-based interventions over extinction-based interventions may be that CC could be more tolerable as it may shift attention away from the experience of fear.

Materials and Methods

Participants

Forty-eight healthy right-handed volunteers (15 males, 33 females; age [22.71±0.44]) with no neurological or psychiatric history, and with normal hearing and normal or corrected-to-normal vision completed the study. Exclusion criteria were pregnancy, disorders of the autonomic system, heart conditions, recreational drug use and any contraindications for MRI. Participants provided written informed consent and were paid 55 euros for their participation. Participants in the CC group were able to earn an additional 14 euros. This study was approved by the local ethical review board (METC Oost-Nederland and CMO Radboudumc). Participants were excluded from the threat acquisition, CC/Extinction, spontaneous recovery, and reinstatement analyses if there was no evidence for successful threat acquisition (mean CS->CS+ or CS+=CS-). For SCRs this was the case for three participants, for PDR this was the case for two participants. Additional participants were excluded in case of missing data due to technical failure.

Design and procedure

This study was a two-day between-subjects experiment carried out in the fMRI scanner (see **Figure 1** for an overview of the design). Participants were assigned to either the CC or Ext group according to a predetermined allocation sequence. At the start of each session, two Ag/AgCl electrodes were attached to the medial phalanges of the second and third digit of the left hand, a pulse oximeter was attached to the first digit of the left hand to measure finger pulse and a respiration belt was placed around the abdomen to measure respiration. All measures were taken using a BrainAmp MR system and recorded using the BrainVision Recorder software (Brain Products GmbH, Munich, Germany). The first day consisted of individual adjustment of the electrical shock followed by a single fMRI session that included the following tasks: an object localizer task (17 min), a category threat conditioning task (23 min) and a CC or extinction task (23 min). The second session took place the following day and consisted of three runs: the spontaneous recovery and reinstatement test (12 min), item recognition test (29 min) and the valence-specific response characterization task (17 min).

Pavlovian conditioning paradigm

Note that CC included an instrumental and not Pavlovian conditioning procedure. This was done because of pragmatic constraints in studies with humans. For example, we cannot food deprive humans to make an appetitive reward truly reinforcing and make participants anticipate the reward. Previous work[50,67] and our pilot studies indicated that to maximize reward anticipation and evoke conditioned responses, the reward conditioning needed to be instrumental.

546 The acquisition, counterconditioning, extinction, spontaneous recovery and reinstatement tasks
547 consisted of a categorical differential delay threat conditioning paradigm[27] with elements of the
548 monetary incentive delay task[30]. Participants viewed trial-unique exemplars of pictures from two
549 categories (animals or objects, see **Figure 1**). In a counter-balanced manner, exemplars from one
550 category served as CS+ (reinforced) stimuli, while exemplars form the other category served as CS-
551 (unreinforced stimuli). Each trial started with the presentation of a stimulus. After a variable delay of
552 2.5-4s, a cue appeared to which participants were instructed to respond as quickly as possible with a
553 button press. After the button press, or when a 1s response window had elapsed, the colour of the
554 cue shifted from black to blue. 0.5-1.5s after the response window elapsed, CS+ items presented
555 during the acquisition phase could be reinforced with a shock. During the acquisition phase, 50% of
556 the CS+ pictures were followed by a shock. After 1s, the stimulus was replaced by neutral feedback
557 during the acquisition, extinction, and recovery tasks. During the CC phase, neutral feedback was
558 replaced by monetary feedback. During the CC phase, participants could obtain a €0.50 reward for
559 their quickest responses to the cues presented on top of CS+ stimuli. The response time target was
560 dynamically adjusted to achieve a reward reinforcement rate of approximately 70%. Reward was
561 withheld during the first three CS+ trials during the CC phase to make the transition from the
562 acquisition to the CC phase more gradual. The inter-trial interval (ITI) varied randomly between 8 and
563 10s. Pictures were presented in a pseudorandom order with no more than 3 consecutive
564 presentations of items from the same category and CC blocks consisted of 40 CS+ and 40 CS-
565 presentations each. The spontaneous recovery block consisted of 15 CS+ and 15 CS+ presentations,
566 and the reinstatement test consisted of 5 CS+ and 5 CS- presentations.

567 ### Item recognition memory test

568 Participants carried out a surprise recognition memory test compromised of 160 pictures (80 CS+, 80
569 CS-) shown during the acquisition and CC/extinction phases, as well as 160 category-matched new
570 items (80 CS+, 80 CS-). Participants rated on a 6-point scale whether the picture was 'definitely old',
571 'probably old', 'maybe old', 'maybe new', 'probably new', 'definitely new'.

572 ### Valence-specific response characterization

573 The valence-specific response characterization task consisted of an adapted version of the
574 conditioning paradigm used during the acquisition phase. Instead of category items, participants
575 were presented with squares in three different colours. One of the stimuli was reinforced with
576 shocks (CS+-shock, 50% reinforcement rate), one stimulus was reinforced with monetary rewards
577 (CS+-reward, approximately 70% reinforcement rate, response time target adjusted dynamically) and
578 the last stimulus was not reinforced (CS-). Each stimulus was presented 40 times in a pseudorandom
579 order with no more than three repetitions of each stimulus. Colours and reinforcement (shocks vs.
580 rewards) were counterbalanced across participants.

581 ### Peripheral stimulation

582 Electrical shocks were delivered using two Ag/AgCl electrodes attached to the medial phalanges of
583 the second and third digit of the right hand using a MAXTENS 2000 (Bio-Protech) device. Shock
584 intensity varied in 10 intensity steps between 0 to 40 V and 0 to 80 mA. Shock duration was 200 ms.
585 In line with prior threat conditioning protocols, shock intensity was calibrated using an ascending
586 staircase procedure starting with a low voltage setting near a perceptible threshold and increasing to
587 a level deemed "maximally uncomfortable but not painful" by the participant[32,73,74].

588 ## Arousal and valence ratings

589 Arousal and valence ratings were acquired using self-assessment manikin scales. The arousal scale
590 ranged from 1 (=extremely calm) to 10 (=extremely excited). The valence scale ranged from 1
591 (=extremely negative) to 10 (=extremely positive). The valence and arousal ratings were collected for
592 the two categories (animals and tools) after the acquisition phase, after the CC/extinction phase, at
593 the start of day 2 immediately before the spontaneous recovery test and after the reinstatement
594 test. For the stimuli used in the valence-specific response characterization task, valence and arousal
595 ratings were collected immediately after the task.

596 ## SCR pre-processing and analysis

597 Electrodermal activity data were pre-processed using in-house software; radio frequency (RF)
598 artefacts were removed and a low-pass filter was applied[75,76]. Skin conductance responses (SCR) were
599 automatically scored with additional, blinded, manual supervision using Autonomate[77]. SCR
600 amplitudes (measured in µSiem) were determined for each trial as the maximum response with an
601 onset between 0.5 and 7.5s after stimulus onset and maximum rise time of 14.5s. Shock- and reward-
602 reinforced trials were excluded from analysis. All response amplitudes were square-root transformed
603 and normalized according to each participant's mean UCS response prior to statistical analysis. The
604 average SCRs were computed per CS-type, task, phase (early, late), and participant.

605 ## PDR pre-processing and analysis

606 Pupil dilation was measured with a MR-compatible eye-tracker from SensoMotoric Instrument (MEye
607 Track-LR camera unit, SMI, SensoMotoric Instruments) and sampled at a rate of 50 Hz. Data were
608 analysed using in-house software[78] implemented in Matlab R2018b (MathWorks), based on
609 previously described methods[79]. Eyeblink artifacts were identified and linearly interpolated 100 ms
610 before and 100 ms after each identified blink. Data from scan runs missing 50% time points or more
611 were excluded. After interpolating missing values, time series were band-pass filtered at 0.05 to 5 Hz
612 (by subtracting the mean and dividing by the standard deviation) within each participant and run to
613 account for between-subjects variance in overall pupil size. Event-related pupil diameter responses
614 were calculated by averaging pupil diameter during 3.5 to 7 sec period after stimulus onset, divided
615 by the 1 sec pre-stimulus pupil diameter (-1 to 0 sec). The average PDRs were computed per CS-type,
616 task, phase (early, late), and participant.

617 ## MRI data acquisition

618 MRI scans were acquired using a Siemens (Erlangen, Germany) 3T MAGNETOM PrismaFit MR scanner
619 equipped with 32-channel transmit-receiver head coil. The manufacturer's automatic 3D-shimming
620 procedure was performed at the beginning of each experiment. Participants were placed in a light
621 head restraint within the scanner to limit head movements during acquisition. Functional images
622 were acquired with multi-band multi-echo gradient echo-planar (EPI) sequence [51 oblique
623 transverse slices; slice thickness, 2.5mm; TR, 1.5s; flip angle, 75°; echo times, 13.4, 34.8, and 56.2 ms;
624 FOV, 210 x 210 mm2; matrix size 84x84x64, fat suppression]. To account for regional variation in
625 susceptibility-induced signal drop out, voxel-wise weighted sums of all echoes were calculated based
626 on local contrast-to-noise ratio after which echo-series are integrated using PAID weighting[80]. Field
627 maps were acquired (51 oblique transverse slices; slice thickness, 2.5mm; TR, 0.49 s; TE, 4.92 ms and
628 7.48 ms; flip angle, 60°; FOV, 210 x 210 mm2; matrix size 84x84x64) at the start of each session to
629 allow for correction of distortions due to magnetic field inhomogeneity. A high-resolution structural
630 image (1mm isotropic) was acquired using a T1-weighted 3D magnetization-prepared rapid gradient

echo sequence [MP-RAGE; TR, 2300 ms; TE, 3.03 ms; flip angle, 8°; 192 contiguous 1 mm slices; FOV = 256 x 256 mm2].

fMRI analysis

Anatomical and functional data were pre-processed using fMRIPrep 20.0.6[81]. The complete boilerplate can be found in Supplementary Information 1. In brief, MRI data were pre-processed in standard stereotactic (MNI152) space. Pulse and respiration data were processed offline using in-house software and visually inspected to remove artefacts and correct peak detection, and corrected pulse and respiration data were used for retrospective image-based correction (RETROICORplus) of physiological noise artefacts in BOLD-fMRI data[82]. Identical transformations were applied to all functional images, which were resliced into 2 mm isotropic voxels. After pre-processing in fMRIPrep, functional images were smoothed with a 6 mm FWHM Gaussian kernel (using SPM12; http://www.fil.ion.ucl.ac.uk/spm; Wellcome Department of Imaging Neuroscience, London, UK).

For the acquisition, extinction/cc and spontaneous recovery phases, BOLD responses to CS+, and CS- during the early phase (first half of the trials) and late phase (second half of the trials) were modelled in 4 separate regressors using box-car functions. Additionally, during all these phases, target presentation, button press and shocks were modelled using stick functions, and feedback presentation and breaks were modelled using box-car functions and included as nuisance regressors. For the category localizer, BOLD responses to animals, objects, and phase-scrambled blocks were modelled in 3 separate regressors using box functions. All first-level models also included six movement parameter regressors (3 translations, 3 rotations) derived from rigid-body motion correction, 25 RETROICOR physiological noise regressors, high-pass filtering (1/128 Hz cut-off), and AR(1) serial correlations correction. First-level contrasts were calculated for early and late CS+ and CS- separately for the acquisition, CC/extinction, and spontaneous recovery phases.

For the acquisition and CC/extinction, first-level contrast were entered into a second-level Group (extinction, cc) x CS-type (CS+, CS-) x Phase (early, late) mixed factorial model using the Multilevel and Repeated Measures (MRM) toolbox[83]. For the spontaneous recovery test, BOLD-responses from the early phase were entered into a second-level Group (extinction, cc) x CS-type (CS+, CS-) mixed factorial model. Thresholding was achieved using nonparametric permutation testing (5,000 iterations), with a cluster-setting threshold of $p<.001$ for whole-brain analysis and familywise error (FWE) correction at $p<0.05$ at cluster-level for whole-brain analysis and voxel-level for ROI-analysis (Amygdala, Hippocampus, vmPFC, NAcc). Activations are displayed on the single-subject high-resolution T1 volume provided by the Montreal Neurological Institute (MNI).

Region of interest definition

Based on a priori hypotheses, results for the amygdala, NAcc, hippocampus and the ventromedial prefrontal cortex are corrected for reduced search volumes using small volume. Masks were created using the WFU PickAtlas toolbox[84] in combination with the Automated Anatomical Labeling atlas[85] for the bilateral amygdala, bilateral hippocampus and vmPFC (Frontal_Med_orb_L&R and Rectus L&R). The *IBASPM 71* anatomical atlas toolbox[86] as used to create a mask for the bilateral NAcc.

Statistical testing

Statistical analyses of behavioural and physiological variables were performed in SPSS (IBM SPSS Statistics Inc.). Dependent measures were submitted to repeated measure ANOVAs and statistics were Greenhouse-Geisser or Huyn-Feldt corrected for non-sphericity when appropriate. Significant findings from ANOVAs were followed-up by paired- and independent samples t-tests. We report

partial eta-square as measure of effect size. Means ± s.e.m are provided where relevant unless otherwise indicated.

Deviations from the pre-registration

The preregistration for this project can be found on OSF (https://osf.io/fbz6n). We pre-registered to sample SCRS in a 0.75 and 3.15 s window after stimulus onset. However, visual inspection of SCR responses during the acquisition phase indicated that response latencies shifted towards the late phase of the trial. We therefore opted to use a longer window (0.5s to 7.5s for stimulus onset) and exclude reinforced trials. The pre-registration erroneously stated that pupil-dilation data would be z-scored and later divided by the pre-stimulus average. PDR data were not z-scored but were only normalized to a 1-sec pre-stimulus baseline. In line with the SCR data, response onset latencies were later than expected. Based on visual inspection of the data from the acquisition phase, we decided to use a window around the expected shock onset: 3.5-7s after stimulus onset. Reinforced trials were excluded. Results for SCR, retrospective reinforcement estimations and the reinstatement test can be found in the **Supplementary Information**. Due to an error in the scripts for the item recognition test, trial-by-trial data were not recorded for the first 12 participants. Therefore, analysis of the memory data focused on averaged data for the early and late phase of acquisition and CC/extinction, leaving out planned change point analyses on bins of 4 trials.

While we planned to extract a vmPFC mask for ROI analysis based on a [CS- > CS+ shock] contrast of BOLD responses during the valence-specific response characterization task to identify “extinction regions”, this did not yield ventromedial prefrontal clusters that survived correction. Instead, in line with our other ROIs, we opted to create a mask based on the AAL atlas. Due to time constraints, native-space and functional connectivity analyses were not carried out for this manuscript.

Data Availability

Pseudonymized data generated in this study are available upon request from the Radboud Data Repository at https://data.ru.nl/. Raw MR images are not publicly available due to privacy or ethical restrictions.

Reference

1 Kessler, R. C. *et al.* Lifetime Prevalence and Age-of-Onset Distributions of. *Arch Gen Psychiatry* **62**, 593-602 (2005).

2 Scheveneels, S., Boddez, Y., Vervliet, B. & Hermans, D. The validity of laboratory-based treatment research: Bridging the gap between fear extinction and exposure treatment. *Behaviour Research and Therapy* **86**, 87-94, doi:10.1016/j.brat.2016.08.015 (2016).

3 Bouton, M. E. Context and behavioral processes in extinction. *Learning and Memory* **11**, 485-494, doi:10.1101/lm.78804 (2004).

4 Myers, K. M. & Davis, M. Behavioral and Neural Analysis of Extinction. *Neuron* **36**, 567-584 (2002).

5 Keller, N. E., Hennings, A. C. & Dunsmoor, J. E. Behavioral and neural processes in counterconditioning: Past and future directions. *Behaviour Research and Therapy* **125**, doi:10.1016/j.brat.2019.103532 (2020).

6 Dickinson, A. & Pearce, J. M. Inhibitory interactions between appetitive and aversive stimuli. *Psychological Bulletin* **84**, 690-711 (1977).

7 Rescorla, R. A. & Solomon, R. L. Two-process learning theory: Relationships between Pavlovian conditioning and instrumental learning. *Psychological Review1* **74**, 151-182 (1967).

8 Pearce, J. M. & Dickinson, A. Pavlovian countercondition: Changing the suppressive properties of shock by association with food. *Animal Behavior Processes* **1**, 170-177 (1975).

9 Kang, S., Vervliet, B., Engelhard, I. M., van Dis, E. A. M. & Hagenaars, M. A. Reduced return of threat expectancy after counterconditioning verus extinction. *Behaviour Research and Therapy* **108**, 78-84, doi:10.1016/j.brat.2018.06.009 (2018).

10 Newall, C., Watson, T., Grant, K. A. & Richardson, R. The relative effectiveness of extinction and counter-conditioning in diminishing children's fear. *Behaviour Research and Therapy* **95**, 42-49, doi:10.1016/j.brat.2017.05.006 (2017).

11 Luck, C. C. & Lipp, O. V. Verbal instructions targeting valence alter negative conditional stimulus evaluations (but do not affect reinstatement rates). *Cognition and Emotion* **32**, 61-80, doi:10.1080/02699931.2017.1280449 (2018).

12 van Dis, E. A. M., Hagenaars, M. A., Bockting, C. L. H. & Engelhard, I. M. Reducing negative stimulus valence does not attenuate the return of fear: Two counterconditioning experiments. *Behaviour Research and Therapy* **120**, 103416, doi:10.1016/j.brat.2019.103416 (2019).

13 Jozefowiez, J. *et al.* Retroactive interference: Counterconditioning and extinction with and without biologically significant outcomes. *Journal of Experimental Psychology: Animal Learning and Cognition* **46**, 443-459, doi:10.1037/xan0000272 (2020).

14 Bouton, M. E. Context, ambiguity, and unlearning: sources of relapse after behavioral extinction. *Biological psychiatry* **52**, 976-986, doi:10.1016/s0006-3223(02)01546-9 (2002).

15 Bouton, M. E. & Peck, C. A. Spontaneous recovery in cross-motivational transfer (counterconditioning). *Animal Learning & Behavior* **20**, 313-321 (1992).

16 Brooks, D. C., Hale, B., Nelson, J. B. & Bouton, M. E. Reinstatement after counterconditioning. *Animal Learning & Behavior* **23**, 383-390, doi:10.3758/BF03198938 (1995).

17 Correia, S. S., McGrath, A. G., Lee, A., Graybiel, A. M. & Goosens, K. A. Amygdala-ventral striatum circuit activation decreases long-term fear. *eLife* **5**, 1-25, doi:10.7554/eLife.12669 (2016).

18 Keller, N. E., Cooper, S. E., McClay, M. & Dunsmoor, J. E. Counterconditioning reduces contextual renewal in a novel context but not in the acquisition context. *Neurobiol Learn Mem* **201**, 107749, doi:10.1016/j.nlm.2023.107749 (2023).

19 Keller, N. E., Hennings, A. C., Leiker, E. K., Lewis-Peacock, J. A. & Dunsmoor, J. E. Rewarded Extinction Increases Amygdalar Connectivity and Stabilizes Long-Term Memory Traces in the vmPFC. *J Neurosci* **42**, 5717-5729, doi:10.1523/JNEUROSCI.0075-22.2022 (2022).

20 Quirk, G. J., Russo, G. K., Barron, J. L. & Lebron, K. The role of ventromedial prefrontal cortex in the recovery of extinguished fear. *Journal of Neuroscience* **20**, 6225-6231, doi:10.1523/jneurosci.20-16-06225.2000 (2000).

21 Morgan, M. A., Romanski, L. M. & LeDoux, J. E. Extinction of emotional learning: Contribution of medial prefrontal cortex. *Neuroscience Letters* **163**, 109-113, doi:10.1016/0304-3940(93)90241-C (1993).

22 Quirk, G. J., Likhtik, E., Pelletier, J. G. & Paré, D. Stimulation of medial prefrontal cortex decreases the responsiveness of central amygdala output neurons. *Journal of Neuroscience* **23**, 8800-8807, doi:10.1523/jneurosci.23-25-08800.2003 (2003).

23 Phelps, E. A., Delgado, M. R., Nearing, K. I. & Ledoux, J. E. Extinction learning in humans: Role of the amygdala and vmPFC. *Neuron* **43**, 897-905, doi:10.1016/j.neuron.2004.08.042 (2004).

24 Dunsmoor, J. E. *et al.* Role of human ventromedial prefrontal cortex in learning and recall of enhanced extinction. *The Journal of Neuroscience* **39**, 2713-2718, doi:10.1523/JNEUROSCI.2713-18.2019 (2019).

25 Diekhof, E. K., Kaps, L., Falkai, P. & Gruber, O. The role of the human ventral striatum and the medial orbitofrontal cortex in the representation of reward magnitude - An activation likelihood estimation meta-analysis of neuroimaging studies of passive reward expectancy and outcome processing. *Neuropsychologia* **50**, 1252-1266, doi:10.1016/j.neuropsychologia.2012.02.007 (2012).

26 Bulganin, L., Bach, D. R. & Wittmann, B. C. Prior fear conditioning and reward learning interact in fear and reward networks. *Frontiers in Behavioral Neuroscience* **8**, 1-11, doi:10.3389/fnbeh.2014.00067 (2014).

27 Dunsmoor, J. E., Martin, A. & LaBar, K. S. Role of conceptual knowledge in learning and retention of conditioned fear. *Biological Psychology* **89**, 300-305, doi:10.1016/j.biopsycho.2011.11.002 (2012).

28 Dunsmoor, J. E. & Kroes, M. C. Episodic memory and Pavlovian conditioning: ships passing in the night. *Current Opinion in Behavioral Sciences* **26**, 32-39, doi:10.1016/j.cobeha.2018.09.019 (2019).

29 Keller, N. E. & Dunsmoor, J. E. The effects of aversive-to-appetitive counterconditioning on implicit and explicit fear memory. *Learning & memory (Cold Spring Harbor, N.Y.)* **27**, 12-19, doi:10.1101/lm.050740.119 (2020).

30 Knutson, B., Westdorp, A., Kaiser, E. & Hommer, D. FMRI visualization of brain activity during a monetary incentive delay task. *NeuroImage* **12**, 20-27, doi:10.1006/nimg.2000.0593 (2000).

31 Dunsmoor, J. E. *et al.* Event segmentation protects emotional memories from competing experiences encoded close in time. *Nature Human Behaviour* (2018).

32 Dunsmoor, J. E., Murty, V. P., Davachi, L. & Phelps, E. A. Emotional learning selectively and retroactively strengthens memories for related events. *Nature* **520**, 345-348, doi:10.1038/nature14106 (2015).

33 Milad, M. R. *et al.* Recall of Fear Extinction in Humans Activates the Ventromedial Prefrontal Cortex and Hippocampus in Concert. *Biological Psychiatry* **62**, 446-454, doi:10.1016/j.biopsych.2006.10.011 (2007).

34 Koizumi, A. *et al.* Fear reduction without fear through reinforcement of neural activity that bypasses conscious exposure. *Nature Human Behaviour* **1**, 1-7, doi:10.1038/s41562-016-0006 (2017).

35 Taschereau-Dumouchel, V. *et al.* Towards an unconscious neural reinforcement intervention for common fears. *Proceedings of the National Academy of Sciences of the United States of America* **115**, 3470-3475, doi:10.1073/pnas.1721572115 (2018).

36 de Voogd, L. D. *et al.* Eye-movement intervention enhances extinction via amygdala deactivation. *Journal of Neuroscience* **38**, 8694-8706, doi:10.1523/JNEUROSCI.0703-18.2018 (2018).

37 Holmes, E. A., James, E. L., Coode-Bate, T. & Deeprose, C. in *PLoS ONE* Vol. 41 (2009).

38 James, E. L. *et al.* Computer Game Play Reduces Intrusive Memories of Experimental Trauma via Reconsolidation-Update Mechanisms. *Psychological Science* **26**, 1201-1215, doi:10.1177/0956797615583071 (2015).

39 Price, R. B., Paul, B., Schneider, W. & Siegle, G. J. Neural correlates of three neurocognitive intervention strategies: A preliminary step towards personalized treatment for psychological disorders. *Cognitive Therapy and Research* **37**, 657-672, doi:10.1007/s10608-012-9508-x (2013).

40 Qin, S., Hermans, E. J., van Marle, H. J. F., Luo, J. & Fernández, G. Acute Psychological Stress Reduces Working Memory-Related Activity in the Dorsolateral Prefrontal Cortex. *Biological Psychiatry* **66**, 25-32, doi:10.1016/j.biopsych.2009.03.006 (2009).

41 Seeley, W. W. *et al.* Dissociable intrinsic connectivity networks for salience processing and executive control. *Journal of Neuroscience* **27**, 2349-2356, doi:10.1523/JNEUROSCI.5587-06.2007 (2007).

42 Liang, X., Zou, Q., He, Y. & Yang, Y. Topologically Reorganized Connectivity Architecture of Default-Mode, Executive-Control, and Salience Networks across Working Memory Task Loads. *Cerebral Cortex* **26**, 1501-1511, doi:10.1093/cercor/bhu316 (2016).

43 Knutson, B. & Cooper, J. C. Functional magnetic resonance imaging of reward prediction. *Current Opinion in Neurology* **18**, 411-417, doi:10.1097/01.wco.0000173463.24758.f6 (2005).

44 Boeke, E. A., Moscarello, J. M., LeDoux, J. E., Phelps, E. A. & Hartley, C. A. Active avoidance: Neural mechanisms and attenuation of pavlovian conditioned responding. *Journal of Neuroscience* **37**, 4808-4818, doi:10.1523/JNEUROSCI.3261-16.2017 (2017).

45 Delgado, M. R., Jou, R. L., LeDoux, J. E. & Phelps, E. A. Avoiding negative outcomes: Tracking the mechanisms of avoidance learning in humans during fear conditioning. *Frontiers in Behavioral Neuroscience* **3**, 1-9, doi:10.3389/neuro.08.033.2009 (2009).

46 Thomas, B. L., Cutler, M. & Novak, C. A modified counterconditioning procedure prevents the renewal of conditioned fear in rats. *Learning and Motivation* **43**, 24-34, doi:10.1016/j.lmot.2012.01.001 (2012).

47 Raczka, K. A. *et al.* Empirical support for an involvement of the mesostriatal dopamine system in human fear extinction. *Translational Psychiatry* **1**, 1-8, doi:10.1038/tp.2011.10 (2011).

48 Thiele, M., Yuen, K. S. L., Gerlicher, A. V. M. & Kalisch, R. A ventral striatal prediction error signal in human fear extinction learning. *NeuroImage* **229**, 117709, doi:10.1016/j.neuroimage.2020.117709 (2021).

49 Esser, R., Korn, C. W., Ganzer, F. & Haaker, J. L-DOPA modulates activity in the vmPFC , nucleus accumbens , and VTA during threat extinction learning in humans. *eLife*, 1-21 (2021).

50 Patil, A., Murty, V. P., Dunsmoor, J. E., Phelps, E. A. & Davachi, L. Reward retroactively enhances memory consolidation for related items. *Learning and Memory* **24**, 65-69, doi:10.1101/lm.042978.116 (2017).

51 Talmi, D., Anderson, A. K., Riggs, L., Caplan, J. B. & Moscovitch, M. Immediate memory consequences of the effect of emotion on attention to pictures. *Learning and Memory* **15**, 172-182, doi:10.1101/lm.722908 (2008).

52 Ballarini, F., Moncada, D., Martinez, M. C., Alen, N. & Viola, H. Behavioral tagging is a general mechanism of long-term memory formation. *Proceedings of the National Academy of Sciences of the United States of America* **106**, 14599-14604, doi:10.1073/pnas.0907078106 (2009).

53 Frey, U. & Morris, R. G. M. Synaptic tagging and long-term potentiation. *Nature* **385**, 533-536 (1997).
54 Braun, E. K., Wimmer, G. E. & Shohamy, D. Retroactive and graded prioritization of memory by reward. *Nature Communications* **9**, 1-12, doi:10.1038/s41467-018-07280-0 (2018).
55 Ambrose, R. E., Pfeiffer, B. E. & Foster, D. J. Reverse Replay of Hippocampal Cells is Uniquely Modulated By Changing Reward. *Neuron* **91**, 1124-1136, doi:10.1016/j.neuron.2016.07.047.Reverse (2018).
56 Foster, D. J. & Wilson, M. A. Reverse replay of behavioural sequences in hippocampal place cells during the awake state. *Nature* **440**, 680-683, doi:10.1038/nature04587 (2006).
57 Diba, K. & Buzsáki, G. Forward and reverse hippocampal place-cell sequences during ripples. *Nature Neuroscience* **10**, 1241-1242, doi:10.1038/nn1961 (2007).
58 Gomperts, S. N., Kloosterman, F. & Wilson, M. A. VTA neurons coordinate with the hippocampal reactivation of spatial experience. *eLife* **4**, 1-22, doi:10.7554/elife.05360 (2015).
59 Gerlicher, A. M. V., Tüscher, O. & Kalisch, R. Dopamine-dependent prefrontal reactivations explain long-term benefit of fear extinction. *Nature Communications* **9**, doi:10.1038/s41467-018-06785-y (2018).
60 Weiland, B. J., Zucker, R. A., Zubieta, J. K. & Heitzeg, M. M. Striatal dopaminergic reward response relates to age of first drunkenness and feedback response in at-risk youth. *Addiction Biology* **22**, 502-512, doi:10.1111/adb.12341 (2017).
61 Weiland, B. J. *et al.* Relationship between impulsivity, prefrontal anticipatory activation, and striatal dopamine release during rewarded task performance. *Psychiatry Research - Neuroimaging* **223**, 244-252, doi:10.1016/j.pscychresns.2014.05.015 (2014).
62 Schott, B. H. *et al.* Mesolimbic functional magnetic resonance imaging activations during reward anticipation correlate with reward-related ventral striatal dopamine release. *Journal of Neuroscience* **28**, 14311-14319, doi:10.1523/JNEUROSCI.2058-08.2008 (2008).
63 Buckholtz, J. W. *et al.* Mesolimbic dopamine reward system hypersensitivity in individuals with psychopathic traits. *Nature Neuroscience* **13**, 419-421, doi:10.1038/nn.2510 (2010).
64 Singer, A. C. & Frank, L. M. Rewarded Outcomes Enhance Reactivation of Experience in the Hippocampus. *Neuron* **64**, 910-921, doi:10.1016/j.neuron.2009.11.016 (2009).
65 Atherton, L. A., Dupret, D. & Mellor, J. R. Memory trace replay: The shaping of memory consolidation by neuromodulation. *Trends in Neurosciences* **38**, 560-570, doi:10.1016/j.tins.2015.07.004 (2015).
66 Brzosko, Z., Schultz, W. & Paulsen, O. Retroactive modulation of spike timingdependent plasticity by dopamine. *eLife* **4**, 1-13, doi:10.7554/eLife.09685 (2015).
67 Zink, C. F., Pagnoni, G., Martin-skurski, M. E., Chappelow, J. C. & Berns, G. S. Human Striatal Responses to Monetary Reward Depend on Saliency. *Neuron* **42**, 509-517 (2004).
68 Haaker, J., Golkar, A., Hermans, D. & Lonsdorf, T. B. A review on human reinstatement studies: An overview and methodological challenges. *Learning and Memory* **21**, 424-440, doi:10.1101/lm.036053.114 (2014).
69 Chang, C. h. & Maren, S. Early extinction after fear conditioning yields a context-independent and short-term suppression of conditional freezing in rats. *Learning & memory (Cold Spring Harbor, N.Y.)* **16**, 62-68, doi:10.1101/lm.1085009 (2009).
70 Devenport, L. D. Spontaneous recovery without interference: Why remembering is adaptive. *Animal Learning and Behavior* **26**, 172-181, doi:10.3758/BF03199210 (1998).
71 Maren, S. Nature and causes of the immediate extinction deficit: A brief review. *Neurobiology of Learning and Memory* **113**, 19-24, doi:10.1016/j.nlm.2013.10.012 (2014).
72 Myers, K. M., Ressler, K. J. & Davis, M. Different mechanisms of fear extinction dependent on length of time since fear acquisition. *Learning and Memory* **13**, 216-223, doi:10.1101/lm.119806 (2006).
73 Kroes, M. C. W., Dunsmoor, J. E., Mackey, W. E., McClay, M. & Phelps, E. A. Context conditioning in humans using commercially available immersive Virtual Reality. *Scientific Reports* **7**, 8640, doi:10.1038/s41598-017-08184-7 (2017).

74 LaBar, K. S., Gatenby, J. C., Gore, J. C., LeDoux, J. E. & Phelps, E. A. Human amygdala activation during conditioned fear acquisition and extinction: A mixed-trial fMRI study. *Neuron* **20**, 937-945, doi:10.1016/S0896-6273(00)80475-4 (1998).
75 de Voogd, L. D., Fernández, G. & Hermans, E. J. Disentangling the roles of arousal and amygdala activation in emotional declarative memory. *Social Cognitive and Affective Neuroscience* **11**, 1471-1480, doi:10.1093/scan/nsw055 (2016).
76 de Voogd, L. D., Fernández, G. & Hermans, E. J. Awake reactivation of emotional memory traces through hippocampal-neocortical interactions. *NeuroImage* **134**, 563-572, doi:10.1016/j.neuroimage.2016.04.026 (2016).
77 Green, S. R., Kragel, P. A., Fecteau, M. E. & LaBar, K. S. Development and validation of an unsupervised scoring system (Autonomate) for skin conductance response analysis. *International Journal of Psychophysiology* **91**, 186-193, doi:10.1016/j.ijpsycho.2013.10.015 (2014).
78 Hermans, E. J., Henckens, M. J. A. G., Roelofs, K. & Fernández, G. Fear bradycardia and activation of the human periaqueductal grey. *NeuroImage* **66**, 278-287, doi:10.1016/j.neuroimage.2012.10.063 (2013).
79 Siegle, G. J., Steinhauer, S. R., Stenger, V. A., Konecky, R. & Carter, C. S. Use of concurrent pupil dilation assessment to inform interpretation and analysis of fMRI data. *NeuroImage* **20**, 114-124, doi:10.1016/S1053-8119(03)00298-2 (2003).
80 Poser, B. A., Versluis, M. J., Hoogduin, J. M. & Norris, D. G. BOLD contrast sensitivity enhancement and artifact reduction with multiecho EPI: Parallel-acquired inhomogeneity-desensitized fMRI. *Magnetic Resonance in Medicine* **55**, 1227-1235, doi:10.1002/mrm.20900 (2006).
81 Esteban, O. *et al.* fMRIPrep: a robust preprocessing pipeline for functional MRI. *Nature Methods* **16**, 111-116, doi:10.1038/s41592-018-0235-4 (2019).
82 Glover, G. H., Li, T. Q. & Ress, D. Image-based method for retrospective correction of physiological motion effects in fMRI: RETROICOR. *Magnetic Resonance in Medicine* **44**, 162-167, doi:10.1002/1522-2594(200007)44:1<162::AID-MRM23>3.0.CO;2-E (2000).
83 McFarquhar, M. *et al.* Multivariate and repeated measures (MRM): A new toolbox for dependent and multimodal group-level neuroimaging data. *NeuroImage* **132**, 373-389, doi:10.1016/j.neuroimage.2016.02.053 (2016).
84 Maldjian, J. A., Laurienti, P. J., Kraft, R. A. & Burdette, J. H. An automated method for neuroanatomic and cytoarchitectonic atlas-based interrogation of fMRI data sets. *NeuroImage* **19**, 1233-1239, doi:10.1016/S1053-8119(03)00169-1 (2003).
85 Tzourio-Mazoyer, N. *et al.* Automated anatomical labeling of activations in SPM using a macroscopic anatomical parcellation of the MNI MRI single-subject brain. *NeuroImage* **15**, 273-289, doi:10.1006/nimg.2001.0978 (2002).
86 Alemán-Gómez, Y., Melie-Garcia, L. & Valdés-Hernández, P. A. in *Proceedings of the 12th Annual Meeting of the Organization for Human Brain Mapping* (2006).

Acknowledgement

This work was supported by the European Research Council (ERC-2015-CoG 682591).

Author contributions

M.C.H., J.E.D., J.H., M.J.A.G.H. and E.H. designed the study. M.C.H. and J.V. implemented and conducted the experiment. M.C.H., L.W. and J.V. analysed the results with support of E.H.. L.W. and M.C.H. wrote the paper with contributions from all authors.

Competing interests

The authors declare no competing interests.

Supplementary Information

Valence-specific response characterization

At the end of the experiment, participants underwent a simplified version of the main experimental task, in which category exemplars were replaced by colored squares. This task was used to investigate to what extent sin conductance responses (SCRs) and pupil dilation responses (PDRs) can be used to disentangle anticipation of shock and reward. Participants viewed three different coloured squares and learned that one colour was associated with shocks (CS+S), one colour with rewards (CS+R) and one colour served as CS-. The trial structure was otherwise identical to comparable trials from the acquisition and CC phases. At the end of the task, participants were asked to rate the three stimuli on valence and arousal self-assessment manikin scales (Bradley & Lang, 1994).

During this valence-specific response characterization task, we observed habituation in SCRs over the course of the task (CS-type (CS+ S, CS+ R, CS-) x Phase (early, late) x Group (CC, Ext) rmANOVA, main effect phase: $F(_{1,38})=13.921$, $p=0.001$, $\eta^2=0.268$) and different SCR magnitudes for the three different CS-types (main effect CS-type (CS+S, CS+R, CS-): $F(_{2,76})=78.460$, $p<0.001$, $\eta^2=0.674$). In addition, habituation depended on CS-type (CS-type x Phase interaction: $F(_{2,76})=6.825$, $p=0.002$, $\eta^2=0.152$). During the early phase, SCRs in response to the CS+R and the CS- were not distinguishable ($t(40)=0.115$, $p=0.909$, CS+R: 0.32±0.03, CS-:0.32 ±0.03), while during the late phase, SCRs to the CS+R were larger than the CS- ($t(40)=4.993$, $p<0.001$, CS+R: 0.29±0.03, CS-:0.19±0.02). SCRs to the CS+S were consistently larger than SCRs to the CS+R (early: $t(41)=9.345$, CS+S: 0.62±0.04, $p<0.001$, late: $t(40)=5.952$, $p<0.001$, CS+S: 0.56±0.04) and the CS- (early: $t(40)=10.020$, $p<0.001$, late: $t(4)=10.122$, $p<0.001$). Thus, anticipation of aversive reinforcement (CS+S) led to increased SCRs compared to anticipation of reward (CS+R) and CS- presentation throughout the task. Due to the fact that SCRs performed less well in differentiation between CS+R and CS-, we focused our analyses on PDRs, but report SCR results here as well.

We also observed CS-type dependent differences in PDRs (CS-type (CS+ S, CS+ R, CS-) x Phase (early, late) x Group (CC, Ext) rmANOVA, main effect CS-type (CS+S, CS+R, CS-): $F(_{2,68}=19.783$, $p<0.001$, $\eta^2=0.368$). In comparison to the neutral CS-, both the shock-reinforced CS+ (CS+S) and reward-reinforced CS+ (CS+R) evoked larger PDRs (**Supplementary Figure 1A**, $t(36)=7.071$, $p<0.001$ and $t(26)=4.900$, $p<0.001$ respectively, CS+S: 1.05±0.03, CS+R: 1.04±0.04, CS-: 1.01±0.02). However, reward- and shock anticipation-induced PDRs did not differ statistically ($t(36)=1.146$, $p=0.259$). While both shock anticipation and reward anticipation led to similar increases in PDRs as compared to the neutral condition, valence and arousal ratings indicated that participants experienced shock and reward trials differently. Specifically, the CS+R was rated more positive than the CS- ($t(47)=9.046$, $p<0.001$, CS+R: 7.79±0.14, CS-: 5.96±0.16, **Supplementary Supplementary Figure 1C**), while the CS+S was rated less positive than the CS- ($t(47)=-10.337$, $p<0.001$, CS+S: 2.96±0.25). Participants reported increased arousal to both the CS+S and CS+R as compared to the CS- ($t(47)=4.666$, $p<0.001$ and $t(47)=8.897$, $p<0.001$ respectively, CS+S: 5.42±0.35, CS+R: 6.31±0.21, CS-: 3.33±0.30, **Supplementary Figure 1B**). While it was not possible to distinguish PDRs to the CS+S and CS+R, explicit ratings of arousal were marginally increased for the CS+R as compared to the CS+S ($t(47)=-2.100$, $p=0.041$). In conclusion, the response characterization task showed that while anticipation of reward and shock both generate increased PDRs as compared to the CS-, distinct retrospective valence ratings show the expected directions.

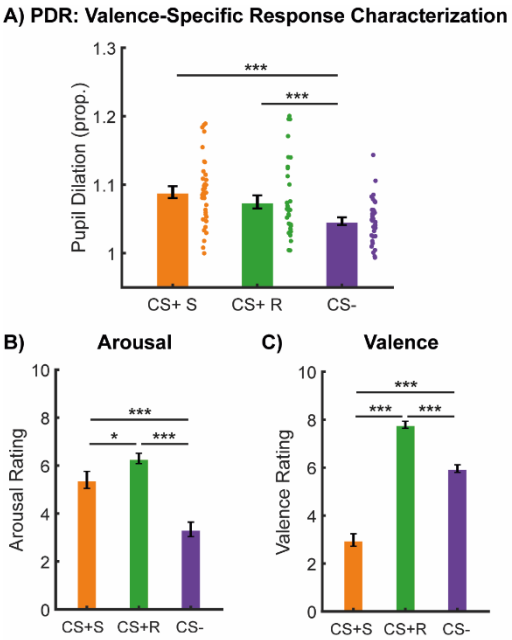

Supplementary Figure 1. Pupil dilation responses (PDRs), explicit arousal and valence rating for the different CSs presented during the valence-specific response characterisation task. (A) PDRs to the shock reinforced (CS+S), reward reinforced (CS+R) and CS- stimuli, averaged across the task and all participants. PDRs were increased for the CS+S and CS+R as compared to the CS- (B) Explicit ratings of arousal and (C) valence provided immediately after the task. Explicit ratings of arousal for the CS+S exceeded ratings for the CS-, and the CS+R was rated higher in arousal than the CS+S. Valence ratings (1=extremely negative, 10=extremely positive) for the CS+R were more positive than ratings for the CS-, while ratings for the CS+S were more negative than for the CS- and CS+R. Error bars represent ± standard error of the mean *=p<0.05, ***=p<0.001

Threat acquisition

Physiological and behavioural evidence for acquisition of conditioned threat responses

Participants pre-assigned to the CC and Ext groups underwent an identical threat acquisition procedure. To verify that participants pre-assigned to both groups acquired conditioned threat responses of comparable strength, we compared PDRs, explicit valence and arousal ratings, and response times between groups. During the acquisition task, participants pre-assigned to both groups showed stable and comparable differential conditioned threat responses as measured by PDRs (**Supplementary Supplementary Figure A,** CS-type (CS+, CS-) x Phase (Early, Late) x Group (CC, Ext) rmANOVA, main effect CS-type: $F_{(1,37)}=41.172$, $p<0.001$, $\eta^2=0.533$, other main effects and interactions: all p's>0.2). Both groups also acquired comparable differential SCRs (main effect CS-type: $F_{(1,42)}=58.633$, $p<0.001$, $\eta^2=0.583$), although SCRs showed habituation over the course of the task (main effect phase: $F_{(1,42)}=66.907$, $p<0.001$, $\eta^2=0.614$, all other p's>0.3). Thus, both SCRs and PDRs demonstrated comparable acquisition of conditioned threat responses between groups.

Successful threat acquisition was further confirmed by valence and arousal ratings for the CS+ and CS- categories at the end of the acquisition task. Arousal ratings for the CS+ category exceeded arousal ratings for the CS- category (**Supplementary Supplementary Figure B**, CS-type (CS+, CS-) x Group (CC, Ext) rmANOVA, main effect CS-type: $F_{(1,44)}=27.573$, $p<0.001$, $\eta^2=0.385$), and did not differ between groups (all p's>0.2). Similarly, the CS+ category was given lower valence (less positive) ratings than the CS- category (**Supplementary Supplementary Figure C**, CS-type (CS+, CS-) x Group (CC, Ext) rmANOVA, main effect CS-type: $F_{(1,44)}=12.626$, $p<0.001$, $\eta^2=0.223$). Although there was no main effect of group on valence ratings (p>0.7), the effect of CS-category unexpectedly differed between the CC and Ext group (CS-type x Group interaction: $F_{(1,44)}=4.512$, $p=0.039$, $\eta^2=0.093$), due to more positive ratings to the CS- category in the Ext group (CC: 5.8±0.4, Ext: 6.9±0.3, $t(44)=2.156$, $p=0.037$). Nevertheless, valence ratings for the CS+ category were comparable between groups (CC: 5.1±0.5, Ext: 4.2±0.4, p>0.1), suggesting that the strength of the acquired threat responses is likely similar between groups.

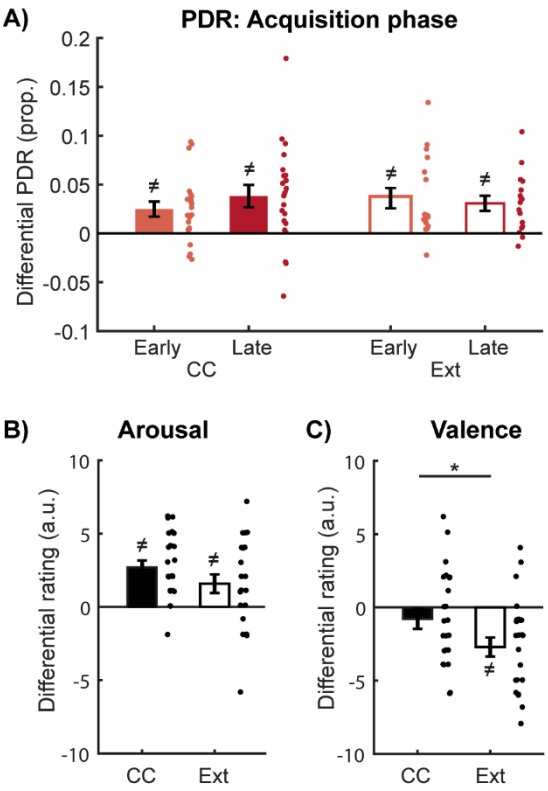

Supplementary Figure 2. Differential PDRs during acquisition and explicit ratings of arousal and valence provided after acquisition. (A) Differential PDRs for the early (light red) and late (dark red) phase of the acquisition task, (B) arousal and (C) valence ratings, displayed separately for participants assigned to the counterconditioning (CC, solid bars) and extinction (EXT, open bars) groups. Both groups showed comparable differential PDRs and arousal ratings during the acquisition task. Participants in both groups showed negative differential valence ratings (stronger negative valence for CS+ vs. CS-), although this effect was stronger in the Ext group. Error bars represent ± standard error of the mean. *, p<0.05. ≠. Significantly different from 0

To keep all experimental tasks similar between groups, participants in both groups were asked to respond to targets that were superimposed on the stimuli as quickly as possible. To verify that both groups performed similarly on this task, we compared response times for the different stimuli between the groups. During the acquisition task, participants responded faster to targets in CS+ trials compared to CS- trials (CS-type (CS+, CS-) x Group (CC, Ext) rmANOVA, main effect CS-type: $F_{(1,45)}=10.839$, $p=0.002$, $\eta^2=0.194$), with no differences between groups (all p's>0.058).

After the acquisition task, participants in both groups reported higher estimated reinforcement rates for the CS+ category as compared to the CS- category (CS-type (CS+, CS-) x Group rmANOVA, main effect CS-type: $F_{(1,45)}=82.176$, $p<0.001$, $\eta^2=0.646$). The reported reinforcement rates did not differ between groups (all p's>0.3).

Brain activation supports successful acquisition of conditioned threat responses

The acquisition of conditioned fear on the first day reliably activated networks associated with fear conditioning. Whole-brain analysis identified regions that were more responsive to the CS+ versus the CS- category (**Supplementary Figure 3**, see **Supplementary Table 1** for a complete overview of findings). We observed differential BOLD responses in a large number of brain areas, including the bilateral insula, posterior and anterior cingulate, thalamus, precuneus (undirected test, cluster size = 425400 mm^3, $p<0.001$, whole-brain FWE-corrected) and the bilateral amygdala (right cluster size = 1088 mm^3, $p<0.001$, FWE-SVC, left cluster size = 736 mm^3, $p<0.001$, FWE-SVC).

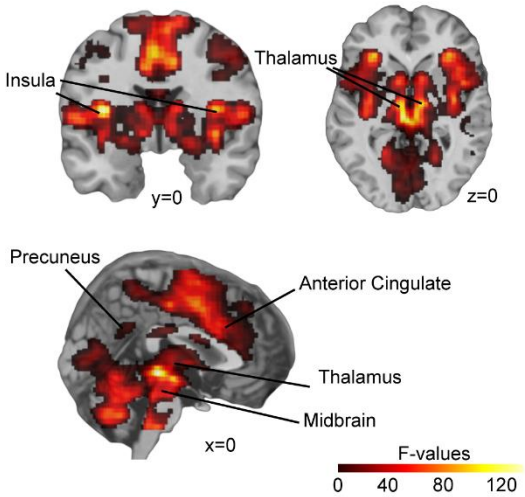

Supplementary Figure 3. Differential threat responses during acquisition revealed CS-specific activation of clusters encompassing a range of regions including the bilateral insula, thalamus, precuneus, anterior cingulate and midbrain. Group F-image of the effect of CS type, thresholded at cluster-level FWE-corrected p<0.05, cluster-forming threshold p=0.001, displayed on the single-subject high-resolution T1 volume provided by the Montreal Neurological Institute (MNI).

Supplementary Table 1. Whole-brain main effects of group (CC, Ext), CS type (CS+, CS-) and phase (early, late) and interactions, during the acquisition task. Cluster-forming threshold p=0.001, FWE-corrected at p<0.05, clusters were labelled using the Talairach Deamon atlas and the AAL atlas for ROIs. For each cluster, the peak voxel coordinates (MNI space) and regions are reported, and additional regions contained within the cluster are added in italics.

		Peak MNI coordinates						
Region	*Cluster*	*x*	*y*	*z*	*Size (mm3)*	*pFWE (cluster)*	*Peak F-value*	*Direction*
CS-type x phase								
Parahippocampa Gyrus L *Insula L, Parahippocamal Gyrus Hippocampus L, Claustrum L, Lentiform Nucleus Putamin L, Uncus L, Postcentral Gyrus BA43 L*	1	-18	-10	-16	6656	0.005	25.86	Early CS+ > Late CS+
Parahippocampa Gyrus Amygdala R *Inferior Frontal Gyrus R, Subcallosal Gyrus BA34R*	2	20	-4	-22	2116	0.033	25.34	
Culmen L *Declive L, Lingual Gyrus L*	3	-8	-54	-16	1720	0.027	20.57	
Parahippocampal Gyrus L *Parahippocampal gyrus BA36L/BA30L, Culmen L*	4	-20	-42	-2	5236	0.006	31.65	
Medial Frontal Gyrus BA11 L *Anterior Cingulate BA32L, Medial Frontal Gyrus BA10 R, BA11 R*	5	-4	38	-14	1104	0.046	17.23	
Superior Temporal Gyrus L *Middle Temporal Gyrus BA21/BA22 L*	6	-52	10	-14	3056	0.015	28.06	
Lingual Gyrus BA18/BA19 R	7	-6	-68	-2	2584	0.018	35.21	
Insula R *Inferior Parietal Lobule R, Superior Temporal Gyrus BA22 R, Postcentral gyrus BA3 R, Superior Temporal Gyrus BA22 R, Precentral Gyrus BA4/BA6, Inferior Parietal Lobule BA40, Middle temporal gyrus, Superior temporal gyrus BA42*	8	38	-6	18	24488	0.001	27.62	
Parahippocampal Gyrus R	9	24	-36	-4	1432	0.035	22.26	
Inferior Frontal Gyrus BA45 R	10	52	14	14	1392	0.036	21.37	
Precentral Gyrus L	11	-60	-8	32	5640	0.006	22.09	
Inferior Parietal Lobule BA40L *Postcentral gyrus BA2L*	12	-56	-36	42	1104	0.046	20.42	
Precuneus L *Postcentral gyrus L, cingulate gyrus L*	13	-14	-42	54	1496	0.034	19.85	

Precuneus R *Paracentral Lobule Ba7 R, Precuneus R, Cingulate gyrus R, Superior Parietal Lobule BA7 R*	14	20	-52	54	5528	0.006	24.86	
Medial Frontal gyrus L (23) *Medial frontal gyrus BA6LR, Paracentral Lobule L*	15	-6	-20	64	1840	0.025	21.47	
CS-type								
Postcentral Gyrus L *Inferior Parietal Lobule LR, Insula LR, Postcentral gyrus R, Cingulate Gyrus LR, Thalamus LR, Caudate LR, Inferior- Middle- and Superior Frontal Gyrus LR, Posterior Cingulate R, Precentral Gyrus LR, Precuneus L, Delice R, Culmen R, Cuneus L, Superior Temporal Gyrus LR, Anterior Cingulate LR, Parahippocampal Gyrus BA27 R, Lentiform nucleus LR*	1	-50	-20	16	425400	<0.001	195.37	CS+>CS-
Posterior Cingulate BA31 L *Precuneus M*	2	-4	-56	24	2816	0.021	26.17	CS+<CS-
Corpus Callosum M *Corpus Callosum R*	3	0	0	22	1296	0.049	35.45	
Angular Gyrus R *Angular Gyrus BA39 R, Precuneus R*	4	56	-66	30	2432	0.024	31.42	
Angular Gyrus BA39L	5	-54	-68	30	5584	0.010	36.02	
Superior Frontal Gyrus BA9L *Superior Frontal Gyrus BA8L, Middle frontal gyrus BA6L*	6	-18	40	42	7200	0.007	33.18	
Phase								
Superior Temporal Gyrus LR, *Inferior Parietal Lobule R, Middle Temporal Gyrus LR, Inferior- Middle- and Superior Frontal Gyrus LR, Caudate LR, Middle Occipital Gyrus LR, Cingulate Gyrus LR, Anterior Cingulate LR, Declive LR, Precuneus LR, Insula LR, Culmen LR, Superior Temporal Gyrus LR, Lingual Gyrus LR, Fusiform Gyrus LR, Angular Gyrus R, Claustrum LR, Thalamus LR, Parahippocampal Gyrus LR, Cuneus LR*	1	-64	-38	12	784632	<0.001	77.44	Early>Late

Counterconditioning and extinction

Skin conductance responses

Differential SCRs were still apparent during the CC/extinction task (CS-type (CS+, CS-) x Phase (Early, Late) x Group (CC, Ext) rmANOVA, main effect CS-type: $F_{(1,40)}=17.609$, $p<0.001$, $\eta^2=0.306$). To verify that successful extinction was reached by the end of the task, we explored SCRs in the late phase separately, but found that differential SCRs were still apparent in that phase ($F_{(1,41)}=12.166$, $p=0.001$, $\eta^2=0.229$). Finally, we explored whether the last two trials of the extinction task showed evidence of residual differential SCRs. In the last two trials of extinction, across both groups, there was no evidence for differential SCRs (all p's>0.2). Thus, while differential SCRs persisted during the late phase of the extinction task, differential responses were no longer apparent in the last two trials. Throughout the CC/extinction, there was no evidence for different SCRs between groups, suggesting that participants in both groups underwent comparable but slow extinction of differential SCRs.

Overlapping stimulus-specific activation during counterconditioning and extinction

A number of clusters showed comparable stimulus-specific activations during CC and extinction (**Supplementary Table 2**).

Supplementary Table 2. **Whole-brain main effect of CS-type during the CC/extinction task.** Cluster-forming threshold p=0.001, FWE-corrected at p<0.05, clusters were labelled using the Talairach Daemon atlas and the AAL atlas for ROIs. For each cluster, the peak voxel coordinates (MNI space) and regions are reported, and additional regions contained within the cluster are added in italics.

Region	*Cluster*	Peak MNI coordinate *x*	*y*	*z*	*Size (mm3)*	*pFWE (cluster)*	*Peak F-value*	*Direction*
CS-type								
Caudate Head L *Thalamus LR, Caudate Head R, Substantia Nigra LR*	1	-10	10	-2	25136	0.001	60.98	CS+>CS-
Insula R *Inferior Frontal Gyrus R, Precentral Gyrus BA44 R, Inferior Frontal Gyrus BA45 R*	3	28	26	0	22800	0.001	89.75	
Inferior Frontal Gyrus L *Insula BA13 L*	4	-32	28	0	7808	0.004	52.01	
Lingual Gyrus L *Inferior Occipital Gyrus L, Cuneus L, Middle Occipital Gyrus L*	5	-24	-80	-12	5696	0.006	32.81	
Superior Temporal Gyrus R *Transverse Temporal Gyrus R*	6	50	-18	6	3744	0.012	30.65	
Lingual Gyrus R *Cuneus R*	7	8	-94	6	3688	0.012	27.81	
Superior Temporal Gyrus L *Transverse temporal Gyrus L*	8	-44	-24	8	3864	0.011	44.50	
Anterior Cingulate BA32 R *Medial Frontal Gyrus BA8 R, Anterior Cingular LR, Cingulate Gyrus BA32 R*	9	4	38	20	7064	0.004	26.61	
Superior Temporal Gyrus R *Supramarginal Gyrus R, Inferior Parietal Lobule BA40R*	10	64	-34	14	3720	0.012	25.88	
Superior Temporal Gyrus L	11	-60	-46	16	2504	0.023	36.62	
Cingulate Gyrus L *Posterior Cingulate BA23R, Posterior Cingulate L*	13	-6	-20	30	3928	0.011	38.33	
Angular Gyrus L *Middle Temporal Gyrus L, Angular Gyrus BA39 L*	12	-44	-64	32	4104	0.010	23.58	CS->CS+
Inferior Temporal Gyrus BA21 L, *Middle Temporal Gyrus BA21 L*	2	-64	-10	-22	1696	0.039	27.05	
Angular Gyrus R *Supramarginal Gyrus R*	14	44	-66	34	1392	0.050	18.35	
Postcentral Gyrus BA40R *Precentral Gyrus Ba4/BA3 R*	15	34	-40	58	1704	0.038	19.84	
Middle Frontal Gyrus BA8/BA6 L	16	-24	16	48	4576	0.008	34.03	

Spontaneous recovery test

Skin conductance responses

To investigate whether CC can prevent spontaneous recovery of differential SCRs, SCRs during the last two trials of extinction and the first two trials of the spontaneous recovery test were submitted to a CS-type (CS+, CS-) x Phase (last 2 trials of the CC/extinction phase, first two trials of the spontaneous recovery test) x Group (CC, Ext) rmANOVA. SCRs showed a generalized increase from the last two trials of extinction to the first two trials of the spontaneous recovery test (main effect phase: $F(1,38)=32.392$, $p<0.001$, $\eta^2=0.460$)). There was evidence for differential SCRs across both phases (main effect CS-type: ($F(1,38)=9.560$, $p=0.004$, $\eta^2=0.201$), as CS+ stimuli evoked higher SCRs than CS- stimuli ($t(43)=2.518$,$p=0.016$, CS+:0.41±0.03, CS-:0.35±0.03), yet we did not find evidence for CS+-specific spontaneous recovery or effect of group (all p's>0.4). Thus, although there was a

generalized increase in responding from the end of extinction to the start of the spontaneous recovery test, SCRs did not show differential recovery and were comparable between groups.

Brain activation

During the spontaneous recovery test, CS-specific activation differed between groups in the inferior temporal gyrus (cluster size = 2008 mm^3, p=0.020, FWE-corrected, **Supplementary Figure 4A**) and the inferior frontal gyrus (cluster size = 1920 mm^3, p=0.022, FWE-corrected, **Supplementary Figure 4B**). Separate analysis of the spontaneous recovery phase within each group did not reveal any suprathreshold clusters in the Ext group, while a number of clusters showed stimulus-specific activation in the CC group. Specifically, the CC group showed stimulus-specific activation in the bilateral fusiform gyri, superior parietal lobes and inferior frontal gyri, and in the right thalamus, caudate, middle frontal gyrus, and angular gyrus (see **Supplementary Table 3)**. A priori defined regions of interest (ROIs) during the spontaneous recovery task were submitted to a Group (CC, Ext) x CS-type (CS+, CS-) x Phase (early, late) rmANOVA but did not reveal any effects.

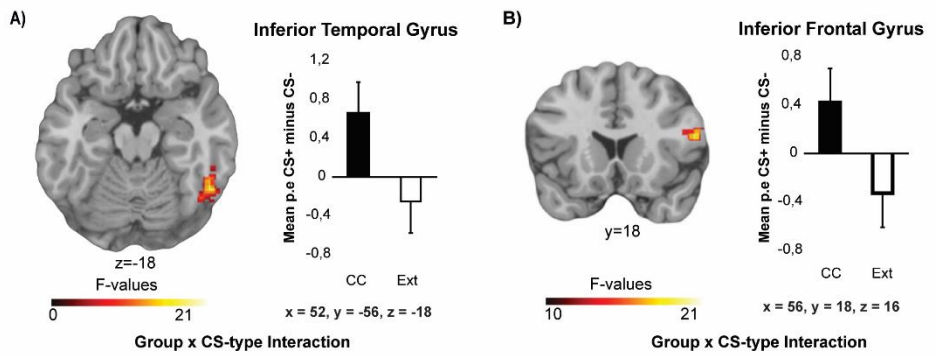

Supplementary Figure 4. During the spontaneous recovery test, stimulus type-specific activation of the inferior temporal and frontal gyri differed between groups. The inferior temporal Gyrus (A) and Inferior frontal gyrus (B) show increased CS+-specific activation in the CC group as compared to the Ext group. Group F-images thresholded at FWE-corrected p<0.05, cluster-forming threshold p=0.001, displayed on the single-subject high-resolution T1 volume provided by the Montreal Neurological Institute (MNI) and parameters estimates from peak voxels.

Supplementary Table 3. Peak voxel coordinates and statistics of activations during the spontaneous recovery phase in the CC group. Clusters were labelled using the AAL atlas. For each cluster, the peak voxel coordinates and regions are reported, and additional regions contained within the cluster are added in italics. Clusters are whole-brain FWE-corrected at p<0.05.

		Peak MNI coordinate						
Region	***Cluster***	***x***	***y***	***z***	***Size (mm3)***	***pFWE (cluster)***	***Peak T-value***	***Direction***
CS-type								
Thalamus R ***Parahippocampal Gyrus R***	1	10	-22	-4	2160	<0.001	6.70	CS+>CS-
Inferior temporal Gyrus R *Fusiform gyrus R*	2	46	-52	-2	4856	<0.001	6.56	
Inferior frontal gyrus, triangular R	3	58	26	26	4992	<0.001	5.93	
Superior parietal lobe R *Angular Gyrus R*	4	26	-60	50	2048	<0.001	5.36	
Inferior frontal gyrus, orbital part L	5	50	26	-6	1120	0.019	5.31	
Fusiform gyrus L *Lingual gyrus*	6	-38	-80	-18	1176	0.015	5.18	
Caudate R	7	6	0	10	1952	<0.001	4.87	
Middle Frontal gyrus R	8	37	0	44	992	0.03	4.86	
Superior parietal lobule L *Angular gyrus L*	9	-32	-58	58	1480	0.004	4.53	

Reinstatement test

SCRs showed a generalized increase from the spontaneous recovery phase to the reinstatement test (CS-type (CS+, CS-) x Group (CC, Ext) x Phase (spontaneous recovery test, reinstatement test) rmANOVA, main effect Phase: $F_{(1,39)}=25.758$, $p<0.001$, $\eta^2=0.398$, last two trials of spontaneous recovery: 0.22±0.04, first two trials of reinstatement: 0.38±0.03). Across the last two trials of the spontaneous recovery test and the first two trials of the reinstatement test, differential SCRs differ between the counterconditioning and extinction group (interaction effect of stimulus type and group: $F_{(1,39)}=4.967$, $p=0.032$, $\eta^2=0.113$). Yet, there is no evidence for differential reinstatement between groups (no CS-type x Phase x Group interaction, $p=0.218$). Moreover, mean SCRs to CS+ and CS- stimuli do not differ within either group (all p's>0.12).

PDRs showed a generalized decrease from the spontaneous recovery phase to the reinstatement test (CS-type (CS+, CS-) x Group (CC, Ext) x Phase (spontaneous recovery test, reinstatement test) rmANOVA, main effect of Phase ($F_{(1,29)}=9.104$, $p=0.005$, $\eta^2=239$)). Mean PDRs decreased from spontaneous recovery to reinstatement ($t(30)=3.063$, $p=0.005$, last two trials of spontaneous recovery: 1.04±0.01, first two trials of reinstatement: 1.01±0.01). Given that we did not observe successful reinstatement in either group, our reinstatement test does not inform us about whether CC can lead to a more persistent attenuation of fear as compared to classic extinction.

CS+-specific enhancement of recognition memory depends on CS+ category

Corrected recognition scores (pHits – pFA) were subjected to a task (acquisition, CC/extinction task) x CS-type (CS+, CS-) x Group (CC, Ext) rmANOVA, including CS+-category (animals, tools) as covariate. Although the effect of CS-type differed depending on the category used as CS+ (CS-type x CS+-category interaction: $F_{(1,42)}=19.400$, $p<0.001$, $\eta^2=0.316$) and task (CS-type x CS+-category x task interaction: $F_{(1,43)}=5.375$, $p=0.025$, $\eta^2=0.113$), showing a stronger effect for tools as CS+, this did not differ between our experimental groups (CS-type x CS+-category x Group interaction: $F(1,41)=0.050$, $p=0.824$; CS-type x task x CS+-category x Group interaction: $F_{(1,41)}=0.005$, $p=0.946$).

To further investigate to what extent CC retroactively affected memory for items presented during the acquisition task, we examined recognition of items presented during acquisition and the CC/extinction tasks separately. Retrospective memory enhancement for the CS+ items compared to CS- items differed depending on the CS+ category during both the acquisition task (CS-type x CS+ category interaction: $F_{(1,42)}=29.730$, $p<0.001$, $\eta^2=0.414$, CS+ category main effect: $F_{(1,42)}=5.346$, $p=0.026$, $\eta^2=0.113$) and the CC/extinction task (CS-type x CS+ category interaction: $F_{(1,42)}=5.121$, $p=0.029$, $\eta^2=0.109$), showing a stronger effect for tools as CS+. Importantly, this effect was comparable between groups (CS-type x CS+ category x Group interaction: acquisition task $F_{(1,41)}=0.016$, $p=0.806$; CC/extinction task $F_{(1,41)}=0.019$, $p=0.890$).